Aus dem
Institut für Kardiovaskuläre Physiologie und Pathophysiologie
Walter-Brendel-Zentrum für Experimentelle Medizin
Institut der Ludwig-Maximilians-Universität München
Vorstand: Prof. Dr. Markus Sperandio

The function of TDP-43 in lymphocyte recruitment

Dissertation
zum Erwerb des Doktorgrades der Medizin
an der Medizinischen Fakultät
der Ludwig-Maximilians-Universität zu München

vorgelegt von
Ruicen Cui
aus
Jilin, China
2021

Mit Genehmigung der Medizinischen Fakultät
der Universität München

Berichterstatter:	Prof. Dr. Markus Sperandio
Mitberichterstatter:	Prof. Dr. Arthur Liesz Prof. Dr. Udo Jeschke
Mitbetreuung durch den promovierten Mitarbeiter:	PD Dr. Heike Beck
Dekan:	Prof. Dr. med. Thomas Gudermann
Tag der mündlichen Prüfung:	25.11.2021

Contents

Contents 3

List of Abbreviations 6

List of figures 9

List of tables 11

Abstract 12

Zusammenfassung 13

1 Introduction 14

1.1 Transactive response DNA binding protein-43 kDa (TARDBP, TDP-43) 14

1.1.1 Structure and function of TDP-43 14

1.1.2 TDP-43 in neurodegenerative diseases 15

1.1.3 TDP-43 in vasculature 17

1.2 Endothelial cells 17

1.2.1 Endothelial cells and vascular tone 18

1.2.2 Endothelium in inflammation 19

1.3 Leukocyte recruitment 19

1.4 Recruitment of lymphocytes 21

1.4.1 Lymphocyte trafficking into the liver 22

1.4.2 Lymphocyte migration into the lung 23

1.4.3 Lymphocyte migration into the spleen 24

1.5 Hypothesis and aim of this thesis 24

2 Materials and Methods 25

2.1 Materials 25

2.1.1 Animals 25

2.1.2 Genotyping 25

2.1.3 Buffers 26

2.1.4 Antibodies 29

2.1.5 Cell line, medium and solutions for cell culture 30

2.1.6 Other drugs and agents used in this thesis 31

2.1.7 Consumables 32
2.1.8 Equipment 32
2.1.9 Software 33
2.2 Methods 34
2.2.1 Mouse Genotyping by PCR 34
2.2.2 Hematoxylin and Eosin (H&E) Staining 36
2.2.3 Periodic Acid Schiff (PAS) Staining 36
2.2.4 Giemsa staining of cremaster muscle 37
2.2.5 Immunofluorescence and confocal microscopy 37
2.2.6 Flow cytometry 38
2.2.7 Assessment of arterial function 40
2.2.8 Intravital microscopy of the mouse cremaster muscle 42
2.2.9 Hematology 44
2.2.10 Cell culture and siRNA transfection 44
2.2.11 Immunoblotting 45
2.2.12 In *vitro* flow chamber assays 47
2.2.13 Statistics 49
3 Results 50
3.1 Generation of TDP-43^{ECKO} mice 50
3.2 Endothelial cell specific knockout of TDP-43 does not influence vascular tone of femoral arteries. 50
3.3 EC-specific deletion of TDP-43 in adult mice leads to massive infiltration of lymphocytes into multiple organs and tissues 54
3.3.1 Macroscopic changes in different organs of TDP-43^{ECKO} mice 54
3.3.2 EC-specific deletion of TDP-43 results in perivascular infiltration of lymphocytes 56
3.3.3 Both, B-lymphocytes and T-lymphocytes contribute to perivascular lymphocyte infiltration in the liver tissue. 58
3.4 Lymphocyte accumulation increased in the liver of TDP-43^{ECKO} mice 58
3.5 EC-specific deletion of TDP-43 and leukocyte recruitment 60

3.6 Knockdown of TDP-43 by siRNA in HUVECs promotes lymphocyte adhesion induced by TNF-α in *vitro*.....61
3.7 Fibronectin expression following TDP-43 silencing in HUVECs....64
3.8 Mice with EC-specific deletion of TDP-43 suffer from anemia, thrombocytopenia and lymphopenia.....65
4 Discussion 66
4.1 Arterial function in TDP-43^{ECKO} mice 67
4.2 Perivascular infiltration of lymphocytes 68
4.3 TDP-43 in endothelial cells regulates leukocyte recruitment in *vivo* 69
4.4 Flow chamber experiments 70
4.6 Outlook 71
References 72
Acknowledgements.....83

List of Abbreviations

ACh:	Acetylcholine
ALS:	Amyotrophic lateral sclerosis
BALT:	Bronchus-associated lymphoid tissue
cAMP:	Cyclic adenosine monophosphate
CFTR:	Cystic fibrosis transmembrane conductance regulator
cGMP:	Cyclic guanosine monophosphate
COX-1:	Cyclooxygenase-1
Ctrl:	Control
EC:	Endothelial cell
ECE:	Endothelin converting enzyme
EDHF:	Endothelium derived hyperpolarizing factor
EDTA:	Ethylenediaminetetraacetic acid
ESAM:	Endothelial cell-selective adhesion molecule
ET-1:	Endothelin-1
ETA:	Endothelin receptor A
ETB:	Endothelin receptor B
FCS:	Fetal calf serum
FTLD:	Frontotemporal lobar degeneration
GTP:	Guanosine triphosphate
HCT:	Hematocrit
HE staining:	Hematoxylin and Eosin Staining
HEV:	High endothelial venules
HGB:	Hemoglobin
HIV-1:	Human immunodeficiency virus type 1
hNFL:	human low molecular weight neurofilament
hnRNP:	Heterogeneous nuclear ribonucleoprotein
hTNFα:	Human tumor necrosis factor-α
HUVECs:	Human umbilical vein endothelial cells
ICAM-1:	Intercellular adhesion molecule 1
INDO:	Indomethacin
IP:	Prostacyclin receptor

ISV:	Intersomitic vessel
JAM-A:	Junctional adhesion molecule A
JAMs:	Junctional adhesion molecule
KO:	Knockout
LFA1:	Lymphocyte function-associated antigen 1
L-NAME:	Nω-Nitro-L-Arginine Methyl-Ester-Hydrochloride
LYMPH:	Lymphocyte
MAC1:	Macrophage antigen 1
MLCK:	Myosin light-chain kinase
MOPS:	3-morpholinopropanesulfone
NE:	Norepinephrine
NEU:	Neutrophil
NO:	Nitric oxide
NOS:	Nitric oxide synthase
PAS staining:	Periodic Acid Schiff Staining
PBS:	Phosphate-buffered saline
PCR:	Polymerase Chain Reaction
PECAM-1:	Platelet endothelial cell adhesion molecule
PGH2:	Prostaglandin H2
PGI2:	Prostacyclin
PKA:	Protein kinase A
PKG:	Protein Kinase G
PLT:	Platelet
PNAd:	Peripheral lymph node addressin
PSGL1:	P-selectin glycoprotein ligand 1
PVDF:	Polyvinylidene difluoride
RBC:	Red blood cell
RET:	Reticulocyte
SDS-PAGE:	Sodium Dodecyl Sulfate Polyacrylamide Gel Electrophoresis
SERs:	Splicing regulatory element
sGC:	Soluble guanylyl cyclase
TBS:	Tris-buffered saline
TBST:	Tris-buffered saline with Tween 20

TDP-43:	Transactive response DNA binding protein 43 kDa
TP:	Thromboxane prostanoid
TXA2:	Thromboxane A2
VAP-1:	Vascular adhesion protein-1
VCAM-1:	Vascular-cell adhesion molecule 1
VLA-4:	Very late antigen-4
VSMC:	Vascular smooth muscle cell
WBC:	White blood cell

List of figures

Figure 1. TDP-43 regulated splicing of CFTR exon 9. 15
Figure 2. TDP-43 under physiological and pathological conditions. 16
Figure 3. Impaired blood circulation and mispatterned vasculature of tardbp-/-; tardbpl-/- double mutants. 17
Figure 4. Leukocyte recruitment cascade (From: Vestweber et al. 2015). 21
Figure 5 Genotyping 35
Figure 6. Gating lymphocyte subsets 39
Figure 7. Model of an isolated femoral artery 41
Figure 8. Cremaster muscle setup for intravital microscopy 43
Figure 9. Setup of micro flow chamber 48
Figure 10. Generation of TDP-43^{ECKO} mice 50
Figure 11. Diameter and vasoconstriction response of isolated femoral arteries 51
Figure 12. Vasodilatory response to ACh 52
Figure 13. Vasodilatory response to Ach following L-NAME and INDO treatment 53
Figure 14. Weight changes of mice 54
Figure 15. Changes in various organs of TDP-43^{ECKO} 55
Figure 16. Increased spleen size in TDP-43^{ECKO} mice compared to control mice 56
Figure 17. TDP-43 deficiency in EC leads to lymphocyte infiltration 57
Figure 18. Fluorescence microscopy of liver sections 58
Figure 19. Lymphocyte populations in different organs 59
Figure 20. EC-specific deletion of TDP-43 increases leukocyte adhesion and decreases rolling velocity in *vivo* 60
Figure 21. Decreased expression of TDP-43 in TDP-43 siRNA treated HUVECs 62
Figure 22. Knockdown of TDP-43 in HUVECs facilitates lymphocyte adhesion 63

Figure 23. Decreased expression of TDP-43 leads to upregulation of fibronectin 64
Figure 24. Total blood cell count 65

List of tables

Table 1. Primers used for genotyping 25
Table 2. Reaction Mixture for Genotyping 26
Table 3. Detailed content of MOPS buffer 26
Table 4. RIPA buffer 26
Table 5. Running Buffer(10X) (1L) 27
Table 6. Blotting Buffer(10X) (1L) 27
Table 7. Blotting Buffer(1X) (1L) 27
Table 8. TBS buffer 10X (pH7.4) (1L) 27
Table 9. TBST buffer (pH7.4) (1L) 27
Table 10. Laemmli buffer 5X (50ml) 28
Table 11. Stacking Gel (5ml) 28
Table 12. Separating Gel (10ml) 28
Table 13. Primary antibodies (H-Human, M-Mouse, R-Rat, Rab-Rabbit) . 29
Table 14. Secondary antibodies 29
Table 15. Medium for HUVECs culture (50ml) 30
Table 16. Cell lysis buffer 30
Table 17. Other drugs and agents 31
Table 18. Consumables for this thesis 32
Table 19. Equipment for this thesis 32
Table 20. Software for this thesis 33
Table 21. Tissue Lysis Buffer 34
Table 22. Detailed PCR protocol for Flox sites 34
Table 23. Detailed PCR protocol for Cre-Recombinase 35

Abstract

TDP-43 is a DNA/RNA binding protein that has multiple functions in gene regulation. So far, studies on TDP-43 mainly focused on its role in neurodegenerative diseases, such as amyotrophic lateral sclerosis and frontotemporal lobar degeneration. However, it was shown that TDP-43 is also involved in the development of the vasculature. Double mutants of TDP-43 in zebrafish resulted in a dramatic mispatterning of blood vessels in both head and trunk. To further analysis this issue, we investigated whether TPD-43 influences vascular function and lymphocyte trafficking in a mouse model. Endothelial cell specific deletion of TDP-43 was achieved by intraperitoneal injection of tamoxifen in $Tardbp^{fl/fl}Cdh5creERT_2$ mice. After that, femoral arteries were isolated to study vessel dilation and vessel constriction. We did not observe a functional role of TDP-43 in arterial dilation and constriction. However, we observed that EC specific loss of TDP-43 in adult mice resulted in massive perivascular lymphocyte infiltration in different organs. In order to study the molecular mechanisms that lead to excessive lymphocyte recruitment, further in *vivo* (cremaster muscle assay) and in *vitro* (micro flow chamber assay) experiments were carried out. In *vivo*, EC specific deletion of TDP-43 facilitated leukocyte adhesion but not leukocyte rolling. In *vitro*, knockdown of TDP-43 in HUVECs promotes lymphocyte adhesion induced by TNF-α. Together, our data demonstrate that TDP-43 expression in ECs plays an important role in regulating lymphocyte recruitment.

Zusammenfassung

TDP-43 ist ein DNA/RNA-Bindungsprotein, das mehrere Funktionen bei der Genregulation erfüllt. Bisher konzentrierten sich die Studien zu TDP-43 hauptsächlich auf seine Rolle bei neurodegenerativen Erkrankungen wie der Amyotrophen Lateralsklerose und frontotemporaler lobärer Degeneration. Es wurde jedoch gezeigt, dass TDP-43 auch an der Entwicklung des Gefäßsystems beteiligt ist. Doppelmutanten von TDP-43 in Zebrafischen zeigten eine dramatische Fehlstrukturierung der Blutgefäße sowohl im Kopf als auch im Rumpf. Ausgehend von diesen Befunden untersuchten wir, welchen Einfluss die Expression von TPD-43 im Endothel auf die Gefäßfunktion hat. Eine endothelzellspezifische Deletion von TDP-43 im Mausmodell wurde durch intraperitoneale Injektion von Tamoxifen erreicht. Danach wurden aus $Tardbp^{fl/fl}Cdh5creERT_2$ Mäusen Femoralarterien isoliert, um Vasodilatation und Vaokonstriktion zu untersuchen. Hier zeigte sich allerdings kein auffälliger Befund. Wir beobachteten jedoch, dass der endothelzell-spezifische knockout von TDP-43 bei den Mäusen zu einer massiven perivaskuären Infiltration von Lymphozyten in verschiedene Organe führte. Daraufhin wurden weitere in *vivo* (Cremaster Muscle Assay) als auch in *vitro* (Micro Flow Chamber Assay) Experimente durchgeführt. Hier konnte ebenfalls gezeigt werden, dass TDP-43 eine wichtige Rolle bei der Regulation der Migration von Lymphozyten spielt. In *vivo* führte die EC-spezifische Deletion von TDP-43 zu einer verstärkten Leukozytenadhäsion an der Gefäßwand, während das Rollen der Leukozyten unverändert blieb. In *vitro* wurde bei TNF-α stimulierten HUVECs ebenfalls eine verstärkte Lymphozytenadhäsion beobachtet, wenn diese weniger TDP-43 exprimierten. Zusammenfassend zeigen die Ergebnisse, dass TDP-43 eine wichtige Rolle bei der Regulierung der Lymphozytenrekrutierung spielt.

1 Introduction

1.1 Transactive response DNA binding protein-43 kDa (TARDBP, TDP-43)

Transactive response DNA-binding protein 43 (TDP-43) was first described based upon its role in binding to TAR, the regulatory element in the human immunodeficiency virus type 1 (HIV-1) long terminal repeat region modulating HIV-1 gene expression (Ou et al. 1995). By binding both DNA and RNA, TDP-43 can also regulate gene splicing (Buratti et al. 2008) and RNA metabolism (Liu et al. 2010). Clinically, TDP-43 was identified as the major disease protein during the development of frontotemporal lobar degeneration (FTLD) and amyotrophic lateral sclerosis (ALS) (Neumann et al. 2006). Moreover, an experimental study in zebrafish revealed that TDP-43 also plays an important role in blood vessel formation (Schmid et al. 2013).

1.1.1 Structure and function of TDP-43

TDP-43 is a ubiquitously expressed protein of 414 amino acids primarily located in the cell nucleus with a molecular weight of 43 kDa (Ou et al. 1995). It is encoded by the TARDBP gene which is located on chromosome 1 and contains 5 coding and 2 noncoding exons (Gendron et al. 2010). The transcript of TDP-43 can be detected in all tissues in humans and rodents (Buratti et al. 2001).

TDP-43 can modulate HIV-1 gene expression. TAR DNA is critical for both Tat-dependent and Tat non-dependent transcriptional regulation of HIV-1. By binding to TAR DNA via ribonucleoprotein-binding domain (RNP), TDP-43 may prevent the binding of TATA binding protein (TBP) to HIV-1 promotor in both the presence and absence of Tat resulting in repression of HIV-1 gene expression (Ou et al. 1995).

TDP-43 has also an important role in the regulation of splicing. Cystic fibrosis transmembrane conductance regulator (CFTR) is a phosphorylation regulated

Cl^- channel. CFTR exon 9 is an alternatively spliced exon. Deletion of exon 9 in human CFTR results in the absence of functional CFTR Cl^- channels (Delaney et al. 1993). (UG)m(u)n regulatory region near the 3'ss is of importance among numerous splicing regulatory elements (SERs) around CFTR exon 9 (Buratti et al. 2001, Buratti et al.2001). Through binding to this region, TDP-43 can recruit heterogeneous nuclear ribonucleoproteins (hnRNP) through its C-tail inhibiting the recognition of splicing factors to this exon (Figure 1, Delaney et al. 1993).

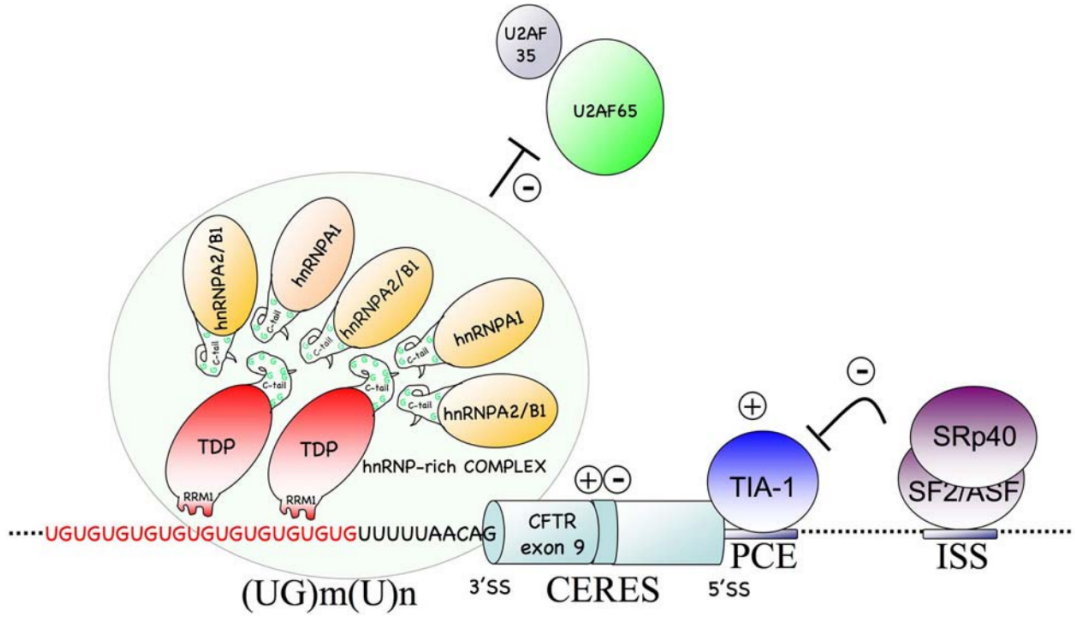

Figure 1. TDP-43 regulated splicing of CFTR exon 9.

By binging to UG repeats region near exon 9, TDP-43 can inhibit the recognition of splicing factors to this region through recruiting hnRNP A/B proteins to the C-tail of TDP-43 (From: Buratti et al. 2008).

1.1.2 TDP-43 in neurodegenerative diseases

Hyper-phosphorylated and ubiquitinated TDP-43 and aggregation of TDP-43 in neurons and/or glial cells are pathological features in FTDL and ALS (Neumann et al. 2006, Arai et al. 2006). Physiologically, TDP-43 is primarily located in the nucleus performing its role in gene expression modulation, gene splicing regulation and mRNA stabilization. Under pathological conditions, however, TDP-43 translocates from its normal position in the nucleus to the cytoplasm

and aggregates (Neumann et al. 2006, Chen et al. 2010). The translocation of TDP-43 to the cytoplasm results in the loss of its normal function and the gain of toxic functions (Figure 2, Chen et al. 2010, Zhang et al. 2009). Arai et al. have shown that TDP-43 inclusions were observed in FTLD and ALS (Arai et al. 2006). Hyperphosphorylation of TDP-43 may lead to abnormal signaling pathways or may influence TDP-43 trafficking directly resulting in dysfunction of neurons and aggregation of ubiquitinated proteins in the cytoplasm. Moreover, both hyper-phosphorylated and ubiquitinated TDP-43 inclusions were observed in cytoplasm of FTLD and ALS (Neumann et al. 2006, Arai et al. 2006). Therefore, hyper-phosphorylated and ubiquitinated aggregates of TDP-43 may play a role in FTLD and ALS.

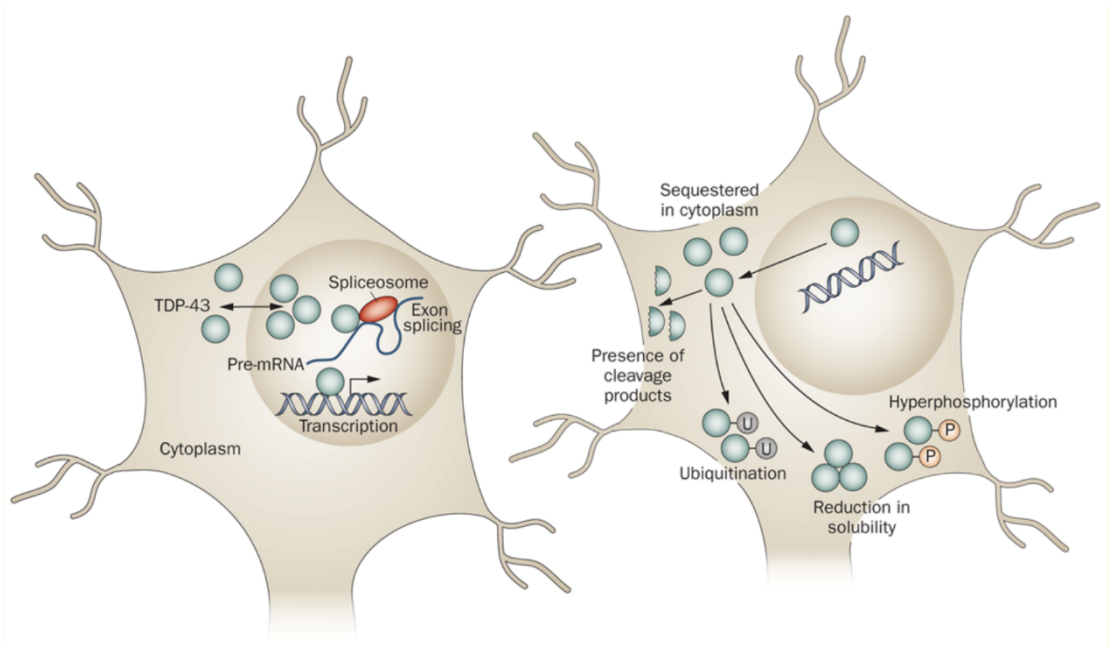

Figure 2. TDP-43 under physiological and pathological conditions.
TDP-43 is primarily located in the nucleus under physiological conditions (left). TDP-43 aggregations with hyper-phosphorylation and /or ubiquitination in the cytoplasm under pathological conditions (right) as observed in FTDL and ALS (From: Chen et al. 2010).

1.1.3 TDP-43 in vasculature

Besides its role in neurodegenerative disorders, TDP-43 also plays an important role in the vascular system. A vascular phenotype was observed by Schmid et al. Double mutant (tardbp$^{-/-}$; tardbpl$^{-/-}$) embryos of zebrafish showed an accumulation of erythrocytes in the yolk sac (Figure 3). In addition, these embryos also displayed a dramatic mispatterning of the intersomitic vessels (ISV) and the head vascular system (Figure 3, Schmid et al. 2013).

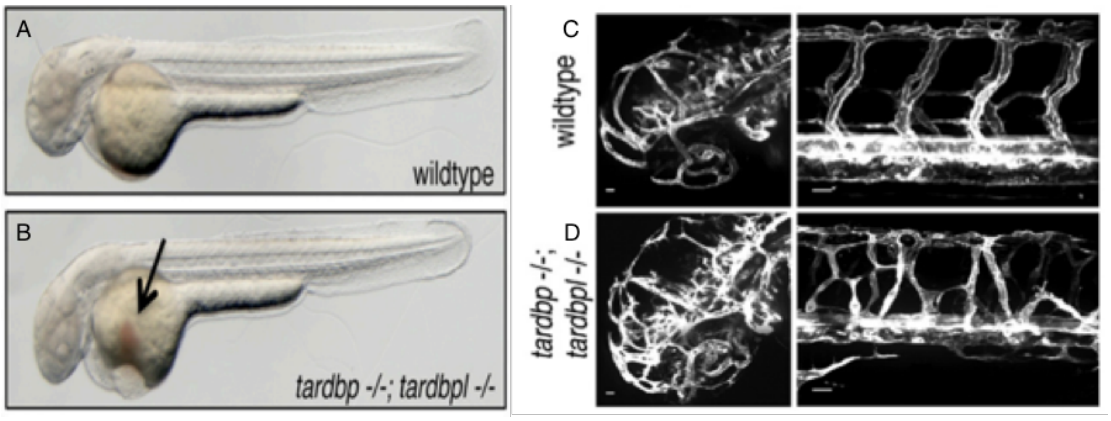

Figure 3. Impaired blood circulation and mispatterned vasculature of tardbp-/-; tardbpl-/- double mutants.
Erythrocytes accumulate in the yolk sac (arrow) in double mutant embryos (B) compared to control (A). The vascular sprouts are super-numerous and hyper-branched in both head (left) vasculature and ISV (right) of zebrafish embryos with double mutants (D) compared to control (C) (From: Schmid et al. 2013).

1.2 Endothelial cells

Endothelial cells (EC) form a continuous mono-layer covering the inner surface of blood vessels and constitute a barrier between the circulating blood and the surrounding tissue (Sato et al. 2001). Endothelial cells line the entire vascular system, from the heart to the smallest capillaries, and show various phenotypes depending on the type of the vessel (Ghitescu et al. 2002). Endothelial cells also play an important role in regulating blood vessel permeability, vascular

tone, inflammation and angiogenesis (Mehta et al. 2006, Sandoo et al. 2010, Pober et al. 2007, Ferrara et al. 2000).

1.2.1 Endothelial cells and vascular tone

ECs release a number of vasoactive substances which regulate vasoconstriction and vasodilation, thereby controling blood pressure. Vasodilators include endothelium derived hyperpolarizing factor (EDHF), nitric oxide (NO) and prostacyclin (PGI_2). Vasoconstrictors include endothelin-1 (ET-1) and thromboxane (TXA_2) (Sandoo et al. 2010).

Constitutive production of nitric oxide (NO) by EC plays an important role in the maintenance of vascular basal tone (Vallance et al. 1989). NO can be formed in ECs from L-arginine by activity of nitric oxide synthase (NOS) after an increase of intracellular Ca^{2+} (Lüscher et al. 1993, Palmer et al. 1988, Bucciet al. 2000). Apart from the increased intracellular Ca^{2+}, phosphorylation of NOS can also increase the production of NO via shear stress (Butt et al. 2000, Boo et al. 2002). Then, NO can rapidly diffuse into adjacent smooth muscle cells (VSMC) across the cell membrane and bind soluble guanylyl cyclase (sGC) which can increase cyclic guanosine monophosphate (cGMP) synthesis from guanosine triphosphate (GTP) (Derbyshire et al.2009). In turn, cGMP activates Protein Kinase G (PKG) which decreases the intracellular calcium levels of VSMCs ultimately leading to relaxation of VSMCs and vasodilation (Yang et al.2005).

Prostacyclin (PGI_2) also plays an important role in vasodilation as an endogenous mediator and is mainly synthesized in the endothelium from arachidonic acid (Spier et al.2007). By binding to prostacyclin receptor (IP) on vascular smooth muscle cells, PGI_2 activates adenylyl cyclase which induces the production of intracellular cyclic adenosine monophosphate (cAMP) (Clapp et al. 2002). cAMP in return activates protein kinase A (PKA) which results in

the relaxation of VSMCs through the phosphorylation of myosin light-chain kinase (MLCK) (Fetalvero et al. 2007, Kamm et al. 1985, Goeckeler et al. 2000).

1.2.2 Endothelium in inflammation

Both infectious agents and tissue damage can cause inflammatory reactions that affect leukocyte and vascular endothelial function with release of cytokines and other pro-inflammatory mediators. Stimulated by mechanical, immunologic and chemical injuries, the activated endothelium upregulates adhesion relevant molecules and increases the secretion of cytokines and other pro-inflammatory factors that allow circulating leukocytes to stick to and finally migrate through the endothelial layer into inflamed tissues (Vestweber et al. 2015, Schmidt et al. 2013).

1.3 Leukocyte recruitment

Leukocyte recruitment into tissues mainly occurs in post capillary venules. It follows a well-defined cascade of adhesion and activation events including capture, rolling, adhesion, crawling and transmigration through the paracellular or transcellular route into tissues (Figure 4, Vestweber et al. 2015).
Leukocyte capture, the initial event, is mediated by selectins and followed by rolling of leukocytes along the endothelium. During this step, endothelial cells play an active role as they express E-selectin and P-selectin which mediate the capture and rolling (McEver et al. 2015). During leukocyte tethering and rolling along the endothelial surface P-selectin and E-selectin interact with P-selectin glycoprotein ligand 1 (PSGL1). P-selectin and E-selectin are primarily expressed on inflamed endothelial cells, whereas L-selectin is expressed by leukocytes. PSGL1 is expressed on most leukocytes but can also be expressed in rare instances on activated endothelial cells (Ley et al. 2007, da Costa Martins et al. 2007).

During rolling, chemokines deposited on inflamed ECs induce leukocyte arrest by activating leukocyte integrins which bind to immunoglobulin superfamily members expressed by endothelial cells, including intracellular adhesion molecule 1(ICAM-1) and vascular cell adhesion molecule 1(VCAM-1) (Campbell et al. 1996). The most important integrins related to leukocyte recruitment are lymphocyte function-associated antigen 1(LFA1/αLβ2 integrin) expressed by all leukocytes, macrophage antigen 1(MAC1/αMβ2 integrin) expressed mostly by myeloid cells and very late antigen 4 (VLA4/α4β1 integrin) expressed by lymphocytes and monocytes (Vestweber et al. 2015).

Transmigration through the vascular wall is the final step of leukocyte recruitment to extravascular tissue. Before transmigration, leukocytes crawl along the endothelium to the exit site with the assistance of MAC1 and ICAM-1 (Phillipson et al. 2006, Barreiro et al. 2003). Leukocytes can transmigrate into tissue either through the trans-endothelial pathway or through the para-cellular pathway (Ley et al. 2007). Various molecules are involved in leukocyte transmigration into tissue involving ICAM-1, JAM-A, PECAM1 and CD99, ESAM, and CD99L2 (Vestweber et al. 2015).

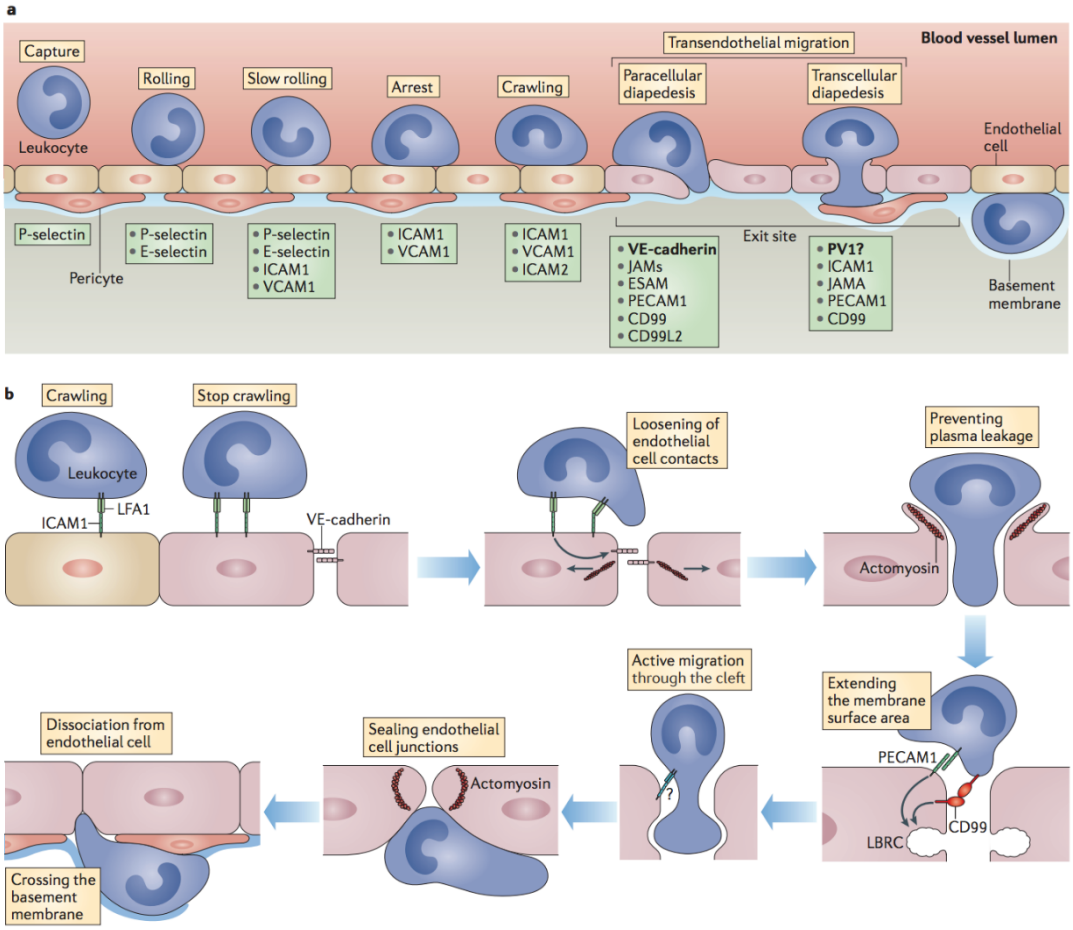

Figure 4. Leukocyte recruitment cascade (From: Vestweber et al. 2015).

1.4 Recruitment of lymphocytes

Lymphocyte recirculation and homing is an essential part of the adaptive immune response that enables foreign antigen recognition in a rapid and specific way. Thus, lymphocytes can recirculate between different sites and migrate into various tissues and organs where they can find their cognate antigen. Transmigration of lymphocytes from blood into tissue primarily occurs in postcapillary venules. Exceptions can be observed in the liver, lung and spleen (Shetty et al. 2008).

1.4.1 Lymphocyte trafficking into the liver

Under physiological conditions, a significant number of lymphocytes resides in the liver. This includes conventional lymphocytes such as B-cells, $CD4^+$ and $CD8^+$ T-cells and unconventional lymphocytes such as NK and NKT cells (Shetty et al. 2008, Racanelli et al. 2006). During inflammation in the liver, lymphocyte recruitment can increase dramatically and infiltrating lymphocytes in the liver are known as important factors that can determine the nature and severity of the disease (Racanelli et al. 2006).

The liver has a unique dual blood supply consisting of vasa privata fed by hepatic arteries and the portal circulation including sinusoidal vessels. The endothelial cells lining sinusoidal vessels show a discontinuous endothelium (Braet et al. 2002).

Lymphocytes can migrate into the liver through several sites such as the portal tracks, the sinusoids and the central hepatic veins (Lalor et al. 2002).
Apart from the structural differences compared to postcapillary venules, hepatic sinusoidal endothelial cells also present unique adhesion molecule expression. Sinusoidal endothelial cells lack the expression of selectins (E-selectin and P-selectin) even under inflammatory conditions (Steinhoff et al. 1993, Adams et al. 1996). Thus, the lack of expression of selectins coupled with the low shear stress in hepatic sinusoids indicates that leukocyte adhesion is selectin-independent in hepatic sinusoids (Lalor et al .2002). Instead, leukocyte recruitment in sinusoidal vessels relies on hyaluronic acid and VCAM-1 (McDonald et al. 2015). Besides VCAM-1, ICAM-1 also supports lymphocyte adhesion to hepatic sinusoids under low shear stress. Studies have shown that blockade of ICAM-1 and VCAM-1 in human sinusoidal endothelial cells results in reduced lymphocyte adhesion to hepatic sinusoids (Edwards et al. 2005, Lalor et al, 2002). Furthermore, vascular adhesion protein 1 (VAP-1) on hepatic sinusoids and α4-integrin on leukocytes also play an essential role for lymphocyte recruitment to the liver. Bonder et al. showed that α4-integrin and

VAP-1 regulate the adhesion of Th1 and Th2 cells to liver sinusoids (Bonder et al. 2005).

Lymphocytes can also infiltrate the portal vessel of the liver. Both CD4 and CD8 positive T cells are found in the portal tract of the normal liver which is important for normal immune surveillance as well as in pathological inflammation (Lalor et al. 2002). Various molecules mediate the recruitment of lymphocytes into the portal tract of the liver under inflammatory or non-inflammatory conditions such as VAP-1 and ICAM-2 (Lalor et al. 1999).

1.4.2 Lymphocyte migration into the lung

Apart from the function in gas exchange, the lung is also critical for the regulation of immune responses to inhaled antigens and microbiota. Lymphocyte accumulation within the lung constitutes a pivotal part in prevention and termination of many pulmonary infectious diseases (Lipscomb et al. 1982). This is supported by specialized lymphocytic tissue in the normal lung termed bronchus-associated lymphoid tissue (BALT) (Bernardo et al. 1990).

Like in the liver, the pulmonary microvasculature has its unique vascular system of capillaries forming an interconnecting network of short vessels which ensures sufficient gas exchange (Aird 2007).

BALT acts as the primary site from where local immune responses are initiated (Randall 2010). Lymphocyte recruitment into BALT from the vasculature depends on the interaction of lymphocytes with high endothelial venules (HEV) (Girard et al. 1995, Xu et al. 2003). Various molecules mediate lymphocyte migration to BALT. In detail, lymphocyte L-selectin/endothelial peripheral lymph node addressin (PNAd) interactions and α4β1/VCAM-1 interactions mediate lymphocytes tethering and rolling on BALT, HEVs and α4β1/VCAM-1 interactions and leukocyte functional antigen (LFA-1) mediate firm adhesion (Xu et al. 2003).

Lymphocyte recruitment to the lung plays an important role in inflammatory pulmonary disease. T-lymphocytes can be selectively recruited into the lung from the vasculature (Lipscomb et al. 1982). In patients, suffering from acute asthma attacks, an increased expression of ICAM-1 on bronchial endothelium was observed (Bentley et al. 1993). Furthermore, endothelial cell loss of ICAM-1 expression in the lung resulted in a 47% reduction in lymphocyte recruitment to the inflamed lung compared with WT mice. Similarly, L-selectin deficient mice also showed reduced lymphocyte recruitment to the inflamed lung (Keramidaris et al. 2001).

1.4.3 Lymphocyte migration into the spleen

The spleen is the largest secondary lymphoid organ that protects against bacterial infection by filtering bacteria from the blood and producing antibodies (Bohnsack et al.1986, Nolte et al. 2002). The spleen is composed of two compartments; the red pulp, which contains blood, and the white pulp, which is full of lymphocytes. The white pulp, also known as the lymphoid region, is composed of the inner T cell zones and the outer B cell follicles. Lymphocytes enter the white pulp from the marginal zone by chemokines and chemokine receptors (Mebius et al. 2005). Spleen does not contain HEV and under normal conditions, lymphocytes enter the spleen from the marginal sinus (Girard et al. 1995, Van Ewijk et al, 1985). Entering of lymphocytes into the spleen requires β2 integrins and α4β1 integrins on lymphocytes and ICAM-1 and VCAM-1 on splenic endothelial cells (Nolte et al. 2002).

1.5 Hypothesis and aim of this thesis

We have conducted this study to investigate the function of endothelial TDP-43 on regulating vascular tone and lymphocyte trafficking hypothesizing that TDP-43 influences such processes. Accordingly, we formulate two aims:
Aim 1: elucidate the role of endothelial TDP-43 in regulating vascular tone.
Aim 2: elucidate the contribution of endothelial TDP-43 in lymphocyte trafficking.

2 Materials and Methods

2.1 Materials

2.1.1 Animals

All animal experiments were conducted in accordance with German Law of Animal Welfare and approved by the Regierung of Oberbayern with the reference numbers AZ. 55.2-1-54-2531-229-15 and 55.2-1-54-2532-172-2015. $Tardbp^{fl/fl}$Cdh5creERT_2 mice (here named TDP-43^{ECKO}) and their respective littermates (control mice) were induced by intraperitoneal tamoxifen injections for three consecutive days to induce Cre recombinase expression and delete TDP-43 in VE-cadherin expressing cells. Deletion of TDP-43 was confirmed by PCR and Western blotting. Mice were maintained and bred at the Institute of Physiology and Cardiovascular Pathophysiology at the Biomedical Center Munich, Ludwig Maximilians Universität, Munich, Germany.

2.1.2 Genotyping

Table 1. Primers used for genotyping

Primer	5′—3′	Company
Cre Forward	GCC TGC ATT ACC GGT CGA TGC AAC GA	Eurofins
Cre Reverse	GTG GCA GAT GGC GCG GCA ACA CCA TT	Genomics
Flox Forward	TGT TGC TTG TTT GCC ATC TT	Eurofins
Flox Reverse	TCT GTA ACT TCA AGA TCT GAC ACC	Genomics

Table 2. Reaction Mixture for Genotyping

Reagent	Volume(μl)
KAPA2G	12.5μl
Forward Primer	2.5μl
Reverse Primer	2.5μl
H_2O	9μl
DNA	1μl

2.1.3 Buffers

Table 3. Detailed content of MOPS buffer

Reagents	Concentration (mM)
CaCl2·2H2O	3.0mM
Mg(SO4)·7H2O	1.17mM
Glucose	5.0mM
NaH2PO4·H2O	1.2mM
EDTA	0.02mM
MOPS	3.0mM
NaCl	145mM
KCl	4.7mM
Pyruvate	2.0mM

Table 4. RIPA buffer

Reagents	Concentration
NaCl	150mM
Tris/HCl	50nM
EDTA	5mM
Na deoxycholate	0.5%
SDS	0.1%
Triton X-100	0.1%

Table 5. Running Buffer(10X) (1L)

Reagents	Weight
Tris base	30.3g
Glycine	144g
SDS	10g
Add distilled H_2O to 1L	

Table 6. Blotting Buffer(10X) (1L)

Reagents	Weight
Tris base	30.3g
Glycine	144g
Add distilled H_2O to 1L	

Table 7. Blotting Buffer(1X) (1L)

Reagents	Weight
Blotting buffer	100ml
Methanol	25ml
Add distilled H_2O to 1L	

Table 8. TBS buffer 10X (pH7.4) (1L)

Reagents	Weight
NaCl	88g
KCl	2g
Tris base	30g
Add distilled H_2O to 1L	

Table 9. TBST buffer (pH7.4) (1L)

Reagents	Weight
10X TBS	100ml
Tween	500 µl
Add distilled H_2O to 1L	

Table 10. Laemmli buffer 5X (50ml)

Reagents	Volume/weight
1M Tris, pH 6.8	15ml
SDS	5g
Glycerin	25ml
β-Mercaptoethanol	10ml
Bromphenol blue	125mg

Table 11. Stacking Gel (5ml)

Reagents	Volume
H_2O	3.4ml
30% acrylamide mix	0.83ml
1M Tris (pH 6.8)	0.63ml
10%SDS	0.05ml
10%ammonium persulfate	0.05ml
TEMED	0.005ml

Table 12. Separating Gel (10ml)

Reagents	Volume
H_2O	3.3ml
30% acrylamide mix	4.0ml
1M Tris (pH 6.8)	2.5ml
10%SDS	0.1ml
10%ammonium persulfate	0.1ml
TEMED	0.004ml

2.1.4 Antibodies

Table 13. Primary antibodies (H-Human, M-Mouse, R-Rat, Rab-Rabbit)

Antibody	labeling	Reactivity	Isotype	Clone	Company
TDP-43	-	H, M, R	Rabbit IgG	Monoclonal	CellSignaling
TGFβ-2	-	H, M, R	Rabbit IgG	Polyclonal	Abcam
VCAM-1	-	H	Rabbit IgG	Monoclonal	CellSignaling
SDF1/CXCL12	-	H, M, R	Rabbit IgG	Monoclonal	CellSignaling
Fibronectin	-	H, M, R	Rabbit IgG	Polyclonal	Abcam
TDP-43	-	H, M, R	Rabbit IgG	Monoclonal	Abcam
Tubulin	-	H, M, R	Mouse IgG1	Monoclonal	Sigma-Aldrich
CD45R/B220	FITC	H, M	Rat IgG2a, κ	Monoclonal	Biolegend
CD3ε	PE	M	Armenian Hamster IgG	Monoclonal	Biolegend
Endomucin	-	M	Rat IgG1k	Monoclonal	Merck
CD3	-	H, M, R	Rabbit IgG	Polyclonal	Abcam
CD45R/B220	PE	H, M	Rat IgG2a, κ	Monoclonal	Thermo Fisher
CD144	-	H	Mouse IgG1	Monoclonal	Thermo Fisher

Table 14. Secondary antibodies

Antibody	Conjugated	Company
Goat anti Human	IRDye® 680RD	LI-COR Biosciences
Goat anti Human	IRDye® 800CW	LI-COR Biosciences
Donkey anti Rat	Alexa Fluor® 488	Invitrogen
Goat anti Rabbit	Alexa Fluor® 546	Invitrogen

2.1.5 Cell line, medium and solutions for cell culture

HUVEC (Human Umbilical Vein Endothelial cells)

Table 15. Medium for HUVECs culture (50ml)

Endothelial Cell Growth Medium	Volume
EGM with Supplement Mix	40ml
Human Serum	10ml

Human serum was thawed at 37^{o}C. For heat inactivation, human serum was kept at 56^{o}C for 30 min. Aliquots of human serum were stored at -20^{o}C .

Table 16. Cell lysis buffer

Reagents	Volume
RIPA	10ml
Protease/Phosphatase inhibitor(100X)	100µl

2.1.6 Other drugs and agents used in this thesis

Table 17. Other drugs and agents

Substance	Company
DMSO	Sigma Aldrich (Deisenhofen, Germany)
SDS	Carl Roth (Karlsruhe, Germany)
Tris	Merck (Darmstadt, Germany)
L-NAME	Sigma Aldrich (Deisenhofen, Germany)
Indomethacine	Sigma Aldrich (Deisenhofen, Germany)
Acetycholine	Sigma Aldrich (Deisenhofen, Germany)
Methanol	AppliChem (Darmstadt, Germany)
Ethanol	Merck (Darmstadt, Germany)
Endothelial cell growth medium	Promocell (Heidelberg, Germany)
MATra-siReagent	Promocell (Heidelberg, Germany)
Universal magnet plate	Promocell (Heidelberg, Germany)
BSA	Capricorn scientific (Ebsdorfergrund, Germany)
7-AAD	BD Biosciences (Piscataway, NJ, USA)
DAPI	AppliChem (Darmstadt, Germany)
Gel Red	Biotium (Hayward, CA, USA)
Gelatine	Custom made
Agarose	Nippon Genetics Europe (Dueren, Germany)
DNA Ladder 100bp	Nippon Genetics Europe (Dueren, Germany)
FBS	Merck (Darmstadt, Germany)
FACS lysing solution	BD Biosciences (Piscataway, NJ, USA)
Glycerin	Merck (Darmstadt, Germany)
Pre-stained Protein Ladder	Li-COR (Lincoln, NE, USA)
Lymphoprep	Alere Technologies AS (Oslo, Norway)
Triton X-100	Sigma Aldrich (Deisenhofen, Germany)
Distilled water	B/BRAUN (Melsungen, Germany)

2.1.7 Consumables

Table 18. Consumables for this thesis

Consumables	Company
Cell strainer 40µm	Greiner (Frickenhausen, Germany)
Filter 0.45µm	Labsolute (Renningen, Germany)
6-Well plate	Falcon, Corning (Corning, NY, USA)
12-Well plate	Falcon, Corning (Corning, NY, USA)
10cm-Culture dish	Falcon, Corning (Corning, NY, USA)
µ-slide VI 0.4	Ibidi (Gräfelfing, Germany)
Tube, 5, 50ml	Falcon, Corning (Corning, NY, USA)
Pipettes 2, 5, 10, 25ml	Greiner (Frickenhausen, Germany)
Syringe 2, 20, 50ml	B/Braun (Melsungen, Germany)

2.1.8 Equipment

Table 19. Equipment for this thesis

Equipment	Company
Intravital microscope BX51W1	Olympus (Hamburg, Germany)
Life cell microscope Axiovert 200M	Zeiss (Jena, Germany)
Optical microscope DM2500 LED	Leica (Wetzlar, Germany)
Gallios Flow cytometer	Beckman Coulter (Krefeld, Germany)
ProCyte DX Hematology analyzer	Idexx (Windsor, UK)
Protein Electrophoresis and blotting	BioRad (California, USA)
Rotina 420R Centrifuge	Merck (Darmstadt, Germany)
pH merter	Mettler Toledo (Greifensee, Switzweland)
Confocoal microscope SP8	Leica (Wetzlar, Germany)
Incubator Galaxy 170S	Eppendorf (Hamburg, Germany)
PCR machine T Advanced	Biometra (Jena, Germany)

2.1.9 Software

Table 20. Software for this thesis

Software	Application	Company
GraphPad Prism8	Statistical analysis	GraphPad (San Diego, CA, USA)
Flowjo	Flow cytometry	BD (San Jose, CA, USA)
Fiji	Image analysis	Bethesda (Maryland, USA)
Image Studio Lite	Western blot	Li-COR (Lincoln, NE, USA)
SigmaPlot	Data analysis	Systat (San Jose, CA, USA)

2.2 Methods

2.2.1 Mouse Genotyping by PCR

In order to determine the genotype of transgenic mice, polymerase chain reaction (PCR) was introduced using the KAPA Mouse Genotyping Kit. Ear or tail samples were harvested and stored at -20^{o}C until DNA extraction. For DNA extraction, 100 µl tissue lysis buffer was added to samples after brief centrifugation and incubation in a thermomixer at 75^{o}C, 900 rpm for 10 minutes followed by 95^{o}C, 900 rpm for 5 minutes. Next, samples were vortexed and centrifuged at highest speed. Then PCR was performed using a PCR machine according to the protocols as indicated below.

Table 21. Tissue Lysis Buffer

Lysis Buffer (100 µl)	Volume(µl)
H_2O	89
Extract Buffer	10
Extract Enzyme	1

Table 22. Detailed PCR protocol for Flox sites

Number of cycles	32	
Initial denaturation	95 °C	3min
Denaturation	95°C	15s
Annealing	57°C	15s
Extension	72°C	15s
Final Extension	72°C	7min

Table 23. Detailed PCR protocol for Cre-Recombinase

Number of cycles	38	
Initial denaturation	95 °C	3min
Denaturation	95°C	15s
Annealing	65°C	15s
Extension	72°C	15s
Final Extension	72°C	7min

Finally, all PCR products were separated on 1.5% agarose-TBE gel containing Gel red to visualize DNA bands. Evaluation was performed under ultraviolet light on a Gel iX2o Imager after electrophoresis in TBE buffer at 120V for 60 minutes (Figure 5).

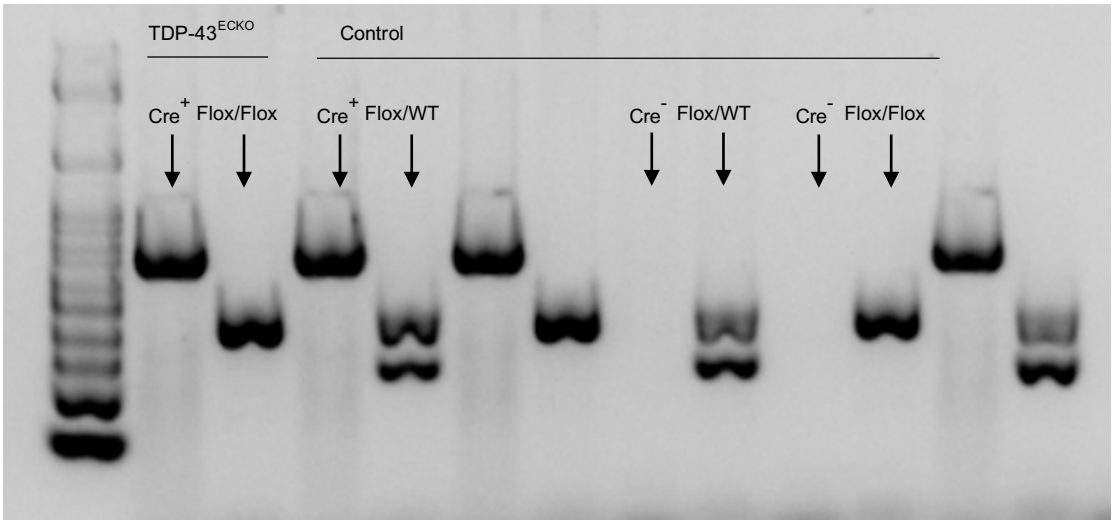

Figure 5 Genotyping

The Figure shows exemplarily various genotypes of mice as determined by PCR. Only one combination (Flox/Flox cre+) represents Tamoxifen-inducible endothelial-cell specific TDP-43 mice (TDP-43^{ECKO} mice). In the blot shown above Flox/Flox (376 bp), Flox/WT (376/230 bp) and cre+ (725 bp) bands were detectable. Mice with the following genotype (TDP-$43^{Flox/Flox}$ X Cre^{-}, TDP-$43^{Flox/WT}$ X Cre^{-} or TDP-$43^{wt/wt}$ X cre^{+} served as control animals. TDP-$43^{Flox/WT}$ X Cre^{+} mice were included in the studies and represent heterozygous endothelial cell specific TDP-43 knockout mice.

2.2.2 Hematoxylin and Eosin (H&E) Staining

Liver, lung and spleen were isolated and fixed in 4% paraformaldehyde overnight followed by immersion in 70% ethanol until embedding in paraffin. Paraffin embedding of tissues was performed using Myr spin tissue processor (STP120, Abacus dx, Australia) using the following protocol:

1. 70% ethanol,1 hour
2. 80% ethanol,1 hour
3. 96% ethanol, two changes,1 hour each
4. 100% ethanol, two changes,1 hour each
5. Xylol, two changes, 1.5 hour each
6. Paraffin wax, two change, 1.5 hour each
7. Embedding tissues into paraffin blocks until use

Then, 8 µm thick paraffin-embedded sections were cut and fixed on slides. After sections had dried on the slides, they were incubated for 2x 10 minutes in xylene for de-paraffinization, 2x 5 minutes 100% ethanol, 2x 5 minutes 96% ethanol, 2x 5 minutes 70% ethanol for re-hydration in the prepared racks. Next the slides were washed in distilled water for 10 minutes. Then the slides were stained in Harris hematoxylin solution for 7 minutes and washed in running tap water for 20 minutes. Slides were then immersed in 1% Eosin solution for 5 minutes followed by another short step of washing in distilled water. Finally, slides were dehydrated through 2x 2 minutes 100% ethanol, cleared in xylene and mounted with xylene soluble mounting medium.

2.2.3 Periodic Acid Schiff (PAS) Staining

Kidney sections were prepared in the same way as for H&E staining. The sections were incubated for 2x 10 minutes in xylene for de-paraffinization, 2x 5 minutes 100% ethanol, 2x 5 minutes 96% ethanol, 2x 5 minutes 70% ethanol for the re-hydration in the prepared racks. Next the slides were washed in distilled water for 10 minutes. Then slides were incubated with 0.5% Periodic acid for 10 minutes followed by washing with distilled water for 5 minutes before

immersion in Schiff reagent for 30 minutes at room temperature followed by washing with running tap water for 5 minutes. After washing, slides were stained with hematoxylin solution for 2 minutes and washed with running tap water for 15 minutes. Finally, slides were dehydrated through 2x 2 minutes 100% ethanol, cleared in xylene and mounted with xylene soluble mounting medium.

2.2.4 Giemsa staining of cremaster muscle

Whole mount cremaster muscles were isolated after in *vivo* experiments and dried on slides. Next, cremaster muscles were fixed by incubating them in 4% PFA for at least 4 hours at 4^{o}C. For staining, cremaster muscles were dried and washed 3x 5 minutes using 0.1M Phosphate Buffer with 5% ethanol. Then, slides were immersed in Giemsa Azur-Eosin-methylene blue solution for 3 minutes at room temperature followed by carefully washing with running tap water and counterstaining with 0.03% acetic acid for 20 minutes. Afterwards, slides were transferred in 70%, 96% and 100% ethanol for 3 minutes. Finally, slides were mounted with xylene soluble mounting medium after incubation with xylene 2x 5 minutes.

2.2.5 Immunofluorescence and confocal microscopy

For the liver, sections were prepared as described in 2.2.2. For antigen retrieval deparaffinized slides were placed into containers containing retrieval solution and the container were heated in heat source (2100 Antigen Retriever, BioVendor, Germany) according to an antigen retrieval program. After that the slides were allowed to cool to room temperature until further processing.
For the HUVECs, cells in ibidi chambers were fixed in 4%PFA followed by washing with PBS 3X5min.
Then, sections were permeabilized with 0.01% Triton for 10 minutes and blocked with1% BSA diluted in PBS for 30 minutes.

After blocking, sections were stained with primary antibodies (TDP-43, CD45R, CD3, Endomucin and VE-Cadherin) diluted in blocking buffer at 4 ^{o}C overnight followed by washing steps with PBS (3x 5 minutes). Next, sections were incubated with the respective secondary antibodies at room temperature for 1 hour followed by washing steps with PBS (3x 5 minutes). DAPI (1:5000, diluted with PBS) was used to stain the nuclei (5 min at room temperature followed by washing steps with PBS (3 x 5 minutes)). Finally, sections were cleaned, dried and mounted with mounting medium. Images were studied and analyzed by use of a SP8 confocal microscope and Fiji Imaging software.

2.2.6 Flow cytometry

2.2.6.1 Cell Harvesting for flow cytometry-spleen, lung, kidney and liver

Spleens, lungs, kidneys and livers were harvested from animals and processed through a cell strainer (40 µm, Thermo Fisher Scientific). Cells were spun down at 1300 RPM for 5min at room temperature. The supernatants were removed and cells were resuspended in 5ml 1% BSA diluted in PBS buffer. Cell counts were performed using a hemocytometer. 10^5 cells were added to flow tubes. Cells were washed by adding 2ml flow cytometry buffer to the flow tubes. After that cells were spun down at 1300 RPM for 5 minutes at room temperature. The supernatant was discarded. Finally, cells were resuspended in 100 µl flow cytometry buffer.

2.2.6.2 Staining

Fluorescence-conjugated antibodies were added to 100 µl cell suspension and mixed by up and down pipetting. Cells were incubated for 30 minutes at 4^{o}C in the dark. After that, cells were washed using flow cytometry buffer and spun down at 1300 RPM at room temperature. Then cells were resuspended in 2ml 1X lysis buffer. Cells were again spun down at 1300 RPM at room temperature and resuspended in 2ml washing buffer to stop the lysis reaction. Finally, cells

were resuspended using Flow cytometry buffer containing 7-AAD and analyzed by flow cytometry using a Gallios Flow Cytometer.

2.2.6.3 Analysis of lymphocyte surface markers

To differentiate T-lymphocytes from B-lymphocytes, antibodies against CD45R and CD3 were used to gate CD45R positive B-cells and CD3 positive T-cells. Surface expression of CD45R and of CD3 of single cells isolated from the organs of TDP-43 knockout and wildtype mice were compared using the Beckman Coulter Gallios^{TM} Flow Cytometer and analysis was performed by FlowJo software (Figure 6).

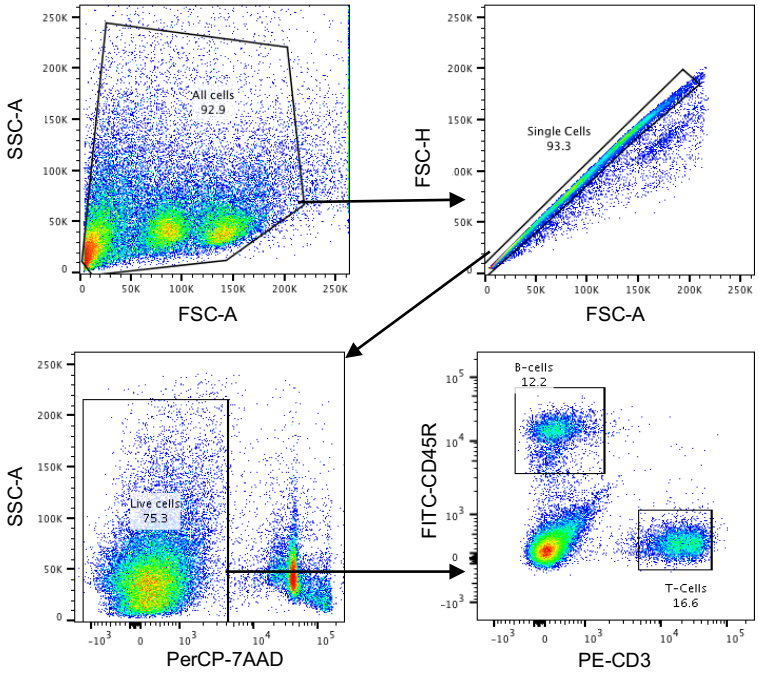

Figure 6. Gating lymphocyte subsets

Cells were prepared as described before and gated as shown. Then lymphocyte subsets were identified by different combinations of antibodies. CD45R was used as a marker of B-lymphocytes and CD3 as a marker of T – lymphocytes.

2.2.7 Assessment of arterial function

2.2.7.1 Isolation and cannulation of femoral arteries

In order to isolate murine femoral arteries, mice were killed by cervical dislocation and legs removed and fixed onto a petri dish coated with silicon for subsequent femoral artery dissection (Figure 7B). Then, the whole femoral arteries were dissected and put in ice-cold MOPS buffer. Ends of isolated arteries were cannulated with glass pipettes as described before (Bolz et al. 1999, Figure 7C). For the cannulation, glass pipettes (GB100F-10:0.58*1.00*100 mm, SCIENCE PRODUCTS GmBH) were pulled into two equally pointed ends using a Laser-Based Micropipette Puller (P-2000, Sutter Instrument, Novato, USA) and fixed on the two sides of a myograph system by screws in suitable position. Next, the two glass pipettes were connected to three way stopcocks using silicone tubing (TYGON® 3350, Pro Liquid). One of the pipettes was considered as the inlet of the vessels and the other was the outlet. The inlet was connected to a 20ml syringe (B/BRAUN, Germany) using an original perfusor line (B/BRAUN, Germany) and filled with MOPS buffer. The inlet was inserted into the proximal end of the isolated femoral artery and fixed with two knots made of 10-0 sutures (Georgia, USA) in order to verify that there is no leakage. After fixation, the blood in the artery was flushed out using MOPS buffer. The other end of the artery was fixed to the outlet glass pipette followed by a leakage test (Figure 7A). Finally, the artery was put into a suitable position for the functional test.

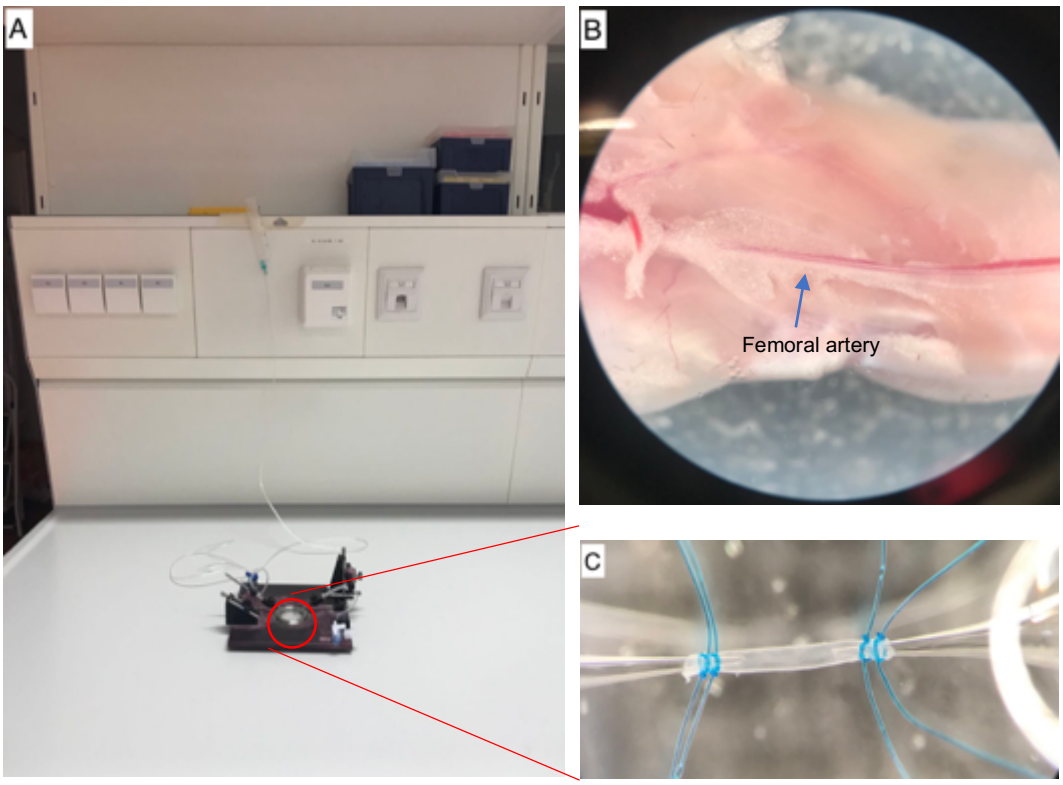

Figure 7. Model of an isolated femoral artery

The syringe was connected with the inlet perfusor line and fixed at a height corresponding to 60mmHg pressure during the experiment. Femoral arteries (B) were freshly isolated and fixed to glass pipettes using 10-0 sutures in the organ bath of the pressure system (C) (Schubert et al. 2017).

2.2.7.2 Norepinephrine (NE) and Acetylcholine (Ach) dose response curves

After fixation of the femoral artery, the system was transported to the stage of a modified inverted microscope (Diaphot 300, Nikon, Düsseldorf, Germany) with a 20x objective (D-APO 20 UV / 340, Olympus) and a video camera (Watec, WAT-902B). The temperature of MOPS Buffer in the organ bath was slowly raised to 37°C. The artery was first treated with 1µM NE followed by incubation with an increasing concentration of Ach (3 nM-10 µM) for 3 minutes. Meanwhile, the outer diameter of the isolated artery was recorded and displayed using BVA software (Hasotec, Rostock, Germany). Then, the artery was washed three times using MOPS Buffer and incubated with 30 µM Nω-nitro-l-arginine methyl

ester (L-NAME) and 30 µM Indomethacine (INDO) for 20 minutes. Finally, the artery was treated with NE and L-NAME as described above.

2.2.8 Intravital microscopy of the mouse cremaster muscle

2.2.8.1 Anesthesia

Mice were anesthetized by intraperitoneal (IP) injection of a combination of Ketaset (12gmg/kg) and Rompun (12.5mg/kg). Therefore, 100 µl Ketaset and 100 µl Rompun were added to 800 µl saline. Anesthesia of mice was induced by a first dose of 100 µl/8g body weight. For maintenance of anesthesia the mice received an additional dose of 100 µl every 1 hour after initiation of anesthesia. Mice were placed on a heating plate to keep the body temperature at around 37^{o}C.

2.2.8.2 Tracheal intubation and carotid artery intubation

After the mice were anesthetized, a plastic tube was inserted into the trachea and fixed using one silk knot in order to keep the respiratory tract unobstructed during the experiment. To administer fluorescent beads, the right carotid artery was catheterized using a plastic tube which was fixed by two silk knots (Figure 8B). Microsurgery was performed on a heating plate under a surgical microscope**.**

2.2.8.3 Preparation of the cremaster muscle

Surgery was performed as described by Baez et al with little modifications. The scrotum was extended moderately and an incision of skin and fascia was made, meanwhile these structures were held up and away from the cremaster muscle using toothed forceps. Next, the cremaster muscle was isolated and an incision was made and extended to the distal end of the scrotum. Then, the cremaster was spread and fixed on a custom-made microscopic stage. The connective tissue was carefully separated from the cremaster muscle by blunt dissection.

During the surgery, any bleeding was stopped by electrocauterization and the cremaster muscle was kept warm and moist (Figure 8C). Finally, the stage was transferred to the microscope in order to start the experiment.

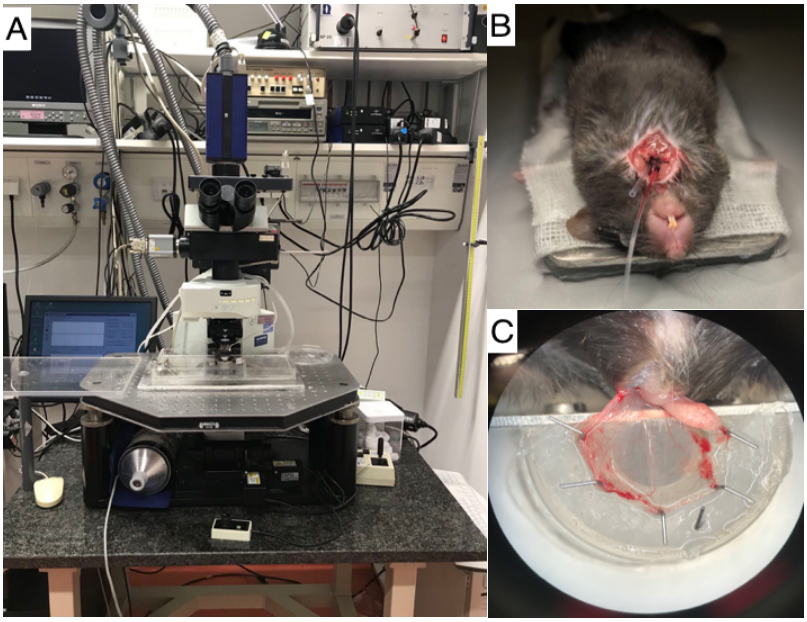

Figure 8. Cremaster muscle setup for intravital microscopy

After surgical preparation of the cremaster muscle, postcapillary venules were studied under the microscope. A: Overview intravital microscope. B: mouse preparation with tracheal intubation and carotid artery catheter. C: cremaster muscle.

2.2.8.4 Leukocyte recruitment

Only postcapillary venules with a dimeter of 20-40 µm were selected for this study. For each mouse, 5 postcapillary venules were chosen and each venule was recorded by intravital microscopy (BX51WI microscope, water immersion objective ×40, 0.80 NA, Olympus; CCD camera, CF8/1, Kappa, Figure 8A) for at least 1 minute. Rolling leukocytes (those moving slower than the associated blood flow), adherent leukocytes (those that remained stationary for 1minute), the leukocyte rolling flux fraction (rolling cells/min divided by total leukocyte flux), rolling velocity, and adherent leukocytes/min (divided by the systemic leukocyte count) were determined.

2.2.9 Hematology

For peripheral blood cell counts whole blood was collected into Heparin treated tubes. Then blood cell counts were measured using Procyte DXcell counter (IDEXX) with mouse hematology settings.

2.2.10 Cell culture and siRNA transfection

Human umbilical vein endothelial cells were kindly isolated by Dorothee Goessel.

2.2.10.1 Cell culture

HUVECs were cultured in an incubator (Galaxy 170S, Eppendorf) at 37 ^{o}C and 5% CO_2. Endothelial cell growth medium was changed every day until passaging and freezing.

HUVECs were cultured in dishes or multi-well-plates until they reached 90% confluency. Then growth medium was removed and cells were washed three times with warm PBS, and incubated with trypsin/EDTA for 1 minute in an incubator (37^{o}C, 5% CO_2). After trypsin/EDTA treatment, 10% FCS (fetal calf serum) was added to the detached cells to stop the enzymatic reaction. Cells were collected and centrifuged at 1000 rpm at room temperature for 5 minutes. Finally, cell pellets were resuspended in growth medium and plated on dishes or multi-well plates.

For cell freezing, cultured HUVECs were treated as described above and transferred into freezing medium (10% DMSO diluted in FCS). They were stored in 1ml aliquots in cryovials at -80°C until further use.
For cell thawing, cryovials were warmed in a water bath to 37^{o}C. Then cells were immediately transferred to warm growth medium. After that, cells were centrifuged (300g, 5min). The supernatant was discarded to remove DMSO.

Finally, cells were resuspended in growth medium and plated on culture dishes and multi-well plates.

2.2.10.2 Transfection

HUVECs were transfected with siRNA against TDP-43 and control siRNA according to the protocol described below.
On the first day, HUVECs (30,000 cells/cm^2) were seeded into 12-well plates containing 1 ml HUVECs growth medium and incubated for 1 hour at 37^oC and 5% CO_2 condition followed by adding 1 ml growth medium. On the second day, the medium was removed and cells were washed using warm PBS 1X. After that PBS was removed and 200 µl Opti-MEM medium was added to each well. In the meantime, the transfection mixture was prepared (1 µg siRNA and 1.2 µl siRNA reagent were added to 50 µl Opti-MEM medium separately and incubated for 5 minutes at room temperature, then mixed thoroughly and incubated at room temperature for 20 minutes). The transfection mixture was added to the cells. Next, 12-well plates were placed on a pre-warmed magnetic plate and incubated for 15 minutes at 37^oC and 5% CO_2. Then the magnetic plate was removed, but the transfection mixture remained for an additional 3-4 hours on the cells. Finally, 2 ml growth medium was added to each well. 72 hours later, cells were harvested and protein lysates were prepared for immunoblotting.

2.2.11 Immunoblotting

2.2.11.1 Preparation of Protein

HUVECs were harvested after three days of siRNA transfection. Cells were washed three times with warm PBS, then incubated with trypsin/EDTA for 1 minute at 37^oC, 5% CO_2. After trypsin/EDTA treatment, 10% FCS was added to the detached cells to stop the enzymatic reaction. The detached cells were transferred to Eppendorf tubes and centrifuged (1,000 rpm, 5 min, room temperature). Next, medium was removed and 100 µl RIPA buffer was added

followed by 10 minutes' incubation on ice. Then the cells were centrifuged at highest speed at 4^{o}C for 10 minutes. The supernatant (100µL) was transferred to a new Eppendorf tube and 25 µl 5xLaemmli buffer was added. Finally, the protein lysates were heated for 5 minutes at 95^{o}C. Samples were cooled down and stored at -80 ^{o}C until further processing.

2.2.11.2 Sodium Dodecyl Sulfate Polyacrylamide Gel Electrophoresis (SDS-PAGE)

Proteins were separated by discontinuous SDS-PAGE using Mini-Protein System (Bio-Rad, Munich, Germany). In order to achieve an optimal separation of proteins, different concentrations of acrylamide in the separating gels were used according to the molecular weight of the proteins of interest**.** Equal amounts of proteins of interest were always loaded on the polyacrylamide gels composed of the separating gel and the stacking gel. Electrophoresis was run at 10 mA per gel for 30 minutes after adding proteins in the pockets, 15 mA per gel for 30 minutes in stacking gel and 25 mA for 75 minutes in separating gel. Protein ladder was used to indicate the molecular weight of the different protein bands.

2.2.11.3 Electroblotting

After the separation of proteins through SDS-PAGE, proteins were electroblotted to a PVDF membrane activated using 25 ml methanol for 15 seconds. After activation of the membrane, it was washed using VE-water for 5 minutes followed by equilibration in blotting buffer for 20 minutes. Then, the PVDF membrane was placed over the gel and clamed in between filter papers and sponge. After the preparation of the blotting cassette, it was mounted in the blotting tank filled with ice-cold blotting buffer and the protein was transferred at 100V for 60 minutes.

2.2.11.4 Antibody staining

After protein transfer, the membrane was first incubated in TBS-Odyssee blocking buffer (1:1) at room temperature for 1 hour to block unspecific proteins. Afterwards, the membrane was incubated with the respective primary antibody diluted in 5 ml Odyssee blocking buffer (1:1000) at 4 ^{o}C overnight. Next, the membrane was washed 3x 5 minutes using TBS buffer and incubated with secondary antibody for 1 hour at room temperature followed by three additional washing steps with TBS-T buffer. Secondary antibodies were diluted in 15 ml Odyssee blocking buffer (1:10000) with 15 µl SDS and 30 µl Tween-20. Finally, the membrane was stored at 4 ^{o}C in TBS-T buffer until imaging, which was performed with Odyssey imaging system and analyzed by Image studio software.

2.2.12 In *vitro* flow chamber assays

2.2.12.1 Preparation of lymphocytes

Human blood samples of 50 ml were collected from healthy donors into a 50 ml syringe (B/Braun, Melsungen, Germany) which was approved by the Regierung of Oberbayern with the reference numbers 611-15. The samples were diluted by adding an equal volume of PBS buffer. Next, 10 ml of diluted blood was carefully layered over 5 ml lymphoprep (Alere Technologies AS, Norway) in 15 ml Falcon tubes avoiding mixing of blood and lymphoprep fluid. This was followed by centrifuging at 800g for 20 minutes at room temperature. After centrifugation, mononuclear cells were removed from the interface between the sample and medium using a glass pipette without removing the upper layer. The harvested cells were diluted with PBS buffer to 50 ml and again centrifuged at 300g for 10 minutes. Subsequently, the supernatant was removed and cells were resuspended with 10 ml PBS buffer followed by cell counting. Finally, the cells were centrifuged at 300g for 10 minutes and diluted to $5x10^5$ cells/ml using HBSS buffer. This cell suspension was used for the flow chamber assays.

2.2.12.2 Preparation of HUVECs coated flow chambers

HUVECs (30.000/cm^2 in 30µl culture medium) were seeded on ibidi chambers (µ-Slide VI 0.4, ibidi, Germany) and were allowed to attach for 2 hours followed by adding 120 µl cell culture medium. On the next day, transfection was carried out according to the protocol described (2.2.10.2). On the third day, flow chamber assays were performed under the microscope. Chambers were either non-treated or treated with 10 ng/ml human TNF-α 4 hours before the flow chamber experiment started.

2.2.12.3 Flow chamber assay

After preparing the lymphocyte suspension, flow chambers (Figure 9B) were perfused with lymphocytes at a wall shear stress of 2 dyn/cm^2 using an infusion pump. In order to maintain a constant flow rate, an infusion pump was used to perfuse cells through the ibidi chamber. Therefore, a tubing was connected to a 20 ml syringe (B/Braun, Germany) (Figure 9A and B). Experiments were recorded 6 minutes using a life cell microscope (Figure 9A). During the experiment, a heating system was used in order to main HUVECs at 37^{O}C. The number of rolling and adherent cells at the 6th minute were assessed using Fiji software.

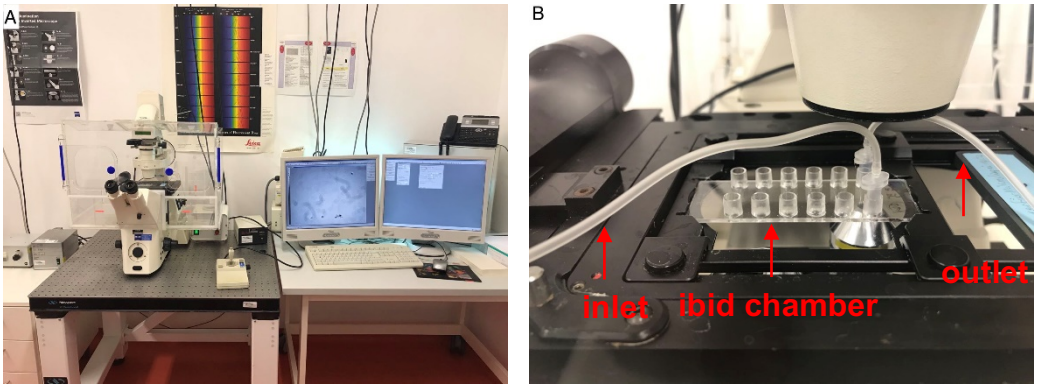

Figure 9. Setup of micro flow chamber

A: Overview life cell microscope system. B: A 20 ml syringe connected to the inlet of an ibidi chamber was used to perfuse the chamber with the lymphocyte suspension with the help of an infusion pump.

2.2.13 Statistics

Data was analyzed using Prism 8 (GraphPad) and presented as mean ± standard error of the mean (mean ± SEM). Unpaired student's t test was used for the comparison between two groups if the data were distributed normally. If the data were not distributed normally, Mann Whitney Rank Sum test was used. Differences were considered statistically significant when a p-value was less than 0.05.

3 Results

3.1 Generation of TDP-43^{ECKO} mice

To investigate the function of TDP-43 expression in endothelial cells, mice with EC-specific deletion of TDP-43 were used in our study. The breeding scheme is shown in Figure 10A. Floxed Tardbp (Tdp43) mice were crossbred with VE-Cadherin-Cre mice to generate TDP-43^{ECKO} mice (Tardbp$^{flox/flox}$; Cre). The genotype of each mouse was analyzed by genotyping (Figure 10B). EC deletion of TDP-43 was induced by intraperitoneal injection of Tamoxifen.

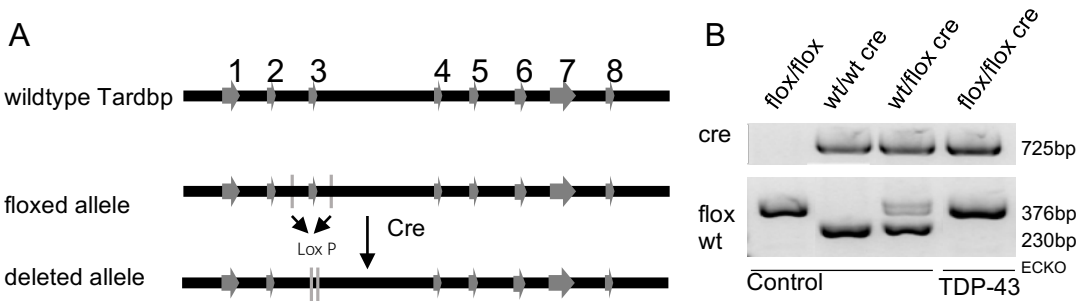

Figure 10. Generation of TDP-43^{ECKO} mice

EC specific TDP-43 deletion strategy (A). Genotyping of ear DNA biopsies (B)

3.2 Endothelial cell specific knockout of TDP-43 does not influence vascular tone of femoral arteries.

To assess the influence of EC specific deletion of TDP-43 in adult mice, we first measured the diameter of femoral arteries immediately after arteries were isolated and fixed in organ bath filled with MOPS buffer. Vasoconstriction responses to NE were then recorded in *vitro*. As displayed in Figure 11, the vasoconstriction response of femoral arteries was not impaired in TDP-43^{ECKO} mice compared to control littermates.

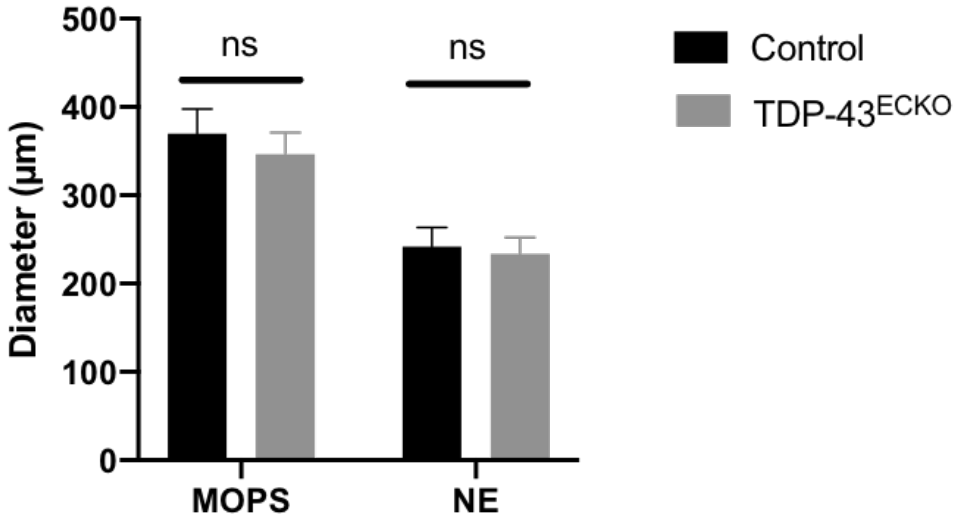

Figure 11. Diameter and vasoconstriction response of isolated femoral arteries

The outer diameter of isolated femoral arteries was measured under 60 mmHg pressure and no significant difference between control and TDP-43^{ECKO} mice could be detected. Constriction response to NE of isolated femoral artery of TDP-43^{ECKO} mice did also not reveal a difference compared with isolated femoral arteries of control mice (control mice n=5, TDP-43^{ECKO} mice n=6, mean ± SEM ns: not significant, unpaired t-test).

Furthermore, the vasodilation response to ACh was investigated in isolated femoral arteries from TDP-43^{ECKO} mice and control animals. Therefore, arteries were fixed as described before and the dilation response was assessed. As displayed in Figure 12, there was no difference in the vasodilatory response to ACh of femoral arteries between TDP-43^{ECKO} and TDP-43^{Ctrl} mice.

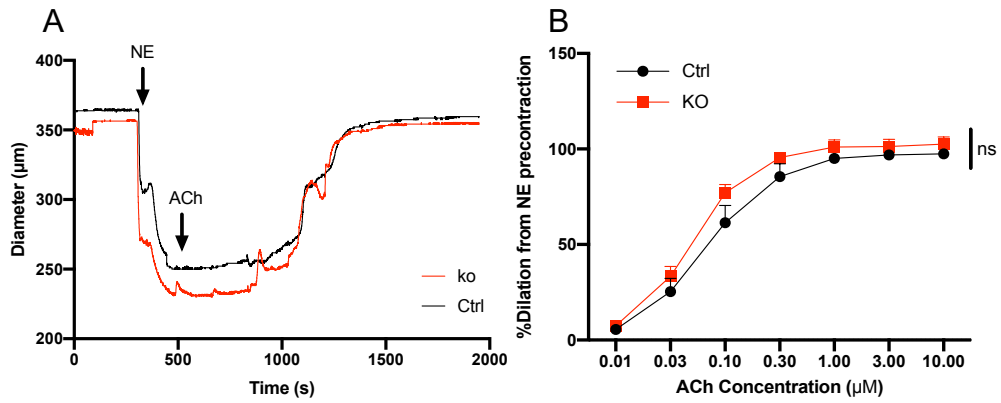

Figure 12. Vasodilatory response to ACh

(A) Diameter recordings of single isolated femoral arteries from KO and WT mice treated with NE and Ach. (B) The vasodilatory responses of femoral arteries from TDP-43^{ECKO} mice to increasing doses of ACh were not statistically different from those observed in control mice. (n=5 mice, mean ± SEM, ns: not significant, t-test)

In order to investigate whether EC specific deletion of TDP-43 can influence vasodilation through NO and PGI-independent and endothelium-mediated pathways, femoral arteries were pre-treated with L-NAME and INDO to inhibit NO and prostaglandin synthesis. Similarly, as shown in Figure 13 no difference in the dilation response to Ach was observed.

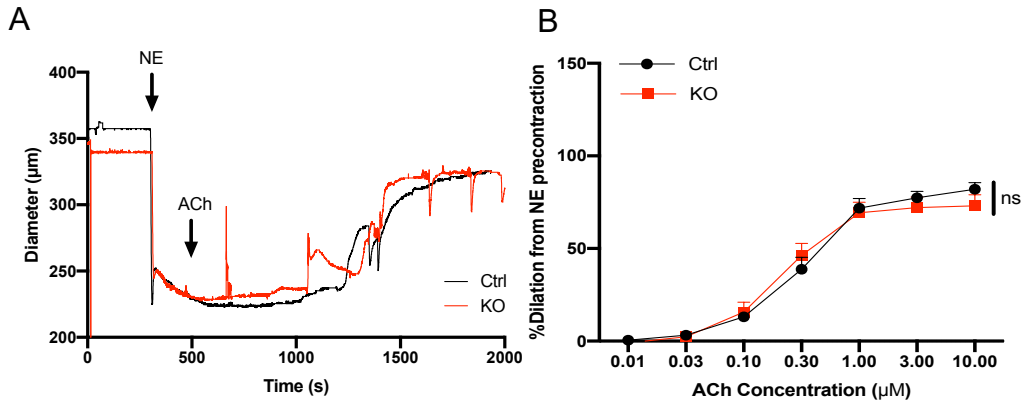

Figure 13. Vasodilatory response to Ach following L-NAME and INDO treatment

(A) Diameter recordings of single isolated femoral arteries from KO and Ctrl mice treated with NE and Ach after L-NAME and INDO incubation. (B) The vasodilatory responses of femoral arteries from TDP-43^{ECKO} mice to increasing doses of Ach was not statistically different from those observed in TDP-43^{Ctrl} mice after L-NAME and INDO treatment. (n=5 mice, mean ± SEM, ns: not significant, t-test).

3.3 EC-specific deletion of TDP-43 in adult mice leads to massive infiltration of lymphocytes into multiple organs and tissues

3.3.1 Macroscopic changes in different organs of TDP-43^{ECKO} mice

We observed that TDP-43^{ECKO} mice suffered from weight loss after tamoxifen injection (Figure 14). Mice were killed if they lost more than 10% weight and organs were examined macroscopically. This revealed a variety of striking visible changes in organs of mice with an EC-specific deletion of TDP-43. Changes were detected in almost all organs and differed in severity and location between the individual mice. As shown in Figure 15, pathologies were observed e.g. on the surface of the liver as well as on the surface of the diaphragm from TDP-43^{ECKO} mice. Most impressively, lungs of TDP-43^{ECKO} mice often lost their normal structure and showed fibrotic changes. The size of the spleen was increased in TDP-43^{ECKO} mice compared to the spleen of control mice as displayed in Figure 16.

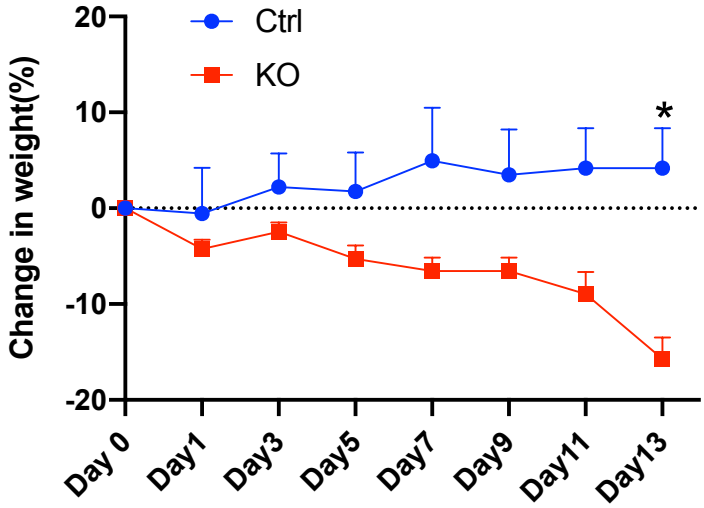

Figure 14. Weight changes of mice

Mice weight was measured from day 0 (first tamoxifen injection) to day 13. TDP-43^{ECKO} mice suffered from weight loss after tamoxifen injection. (n=4 mice, mean ± SEM, * $p<0.05$, t-test)

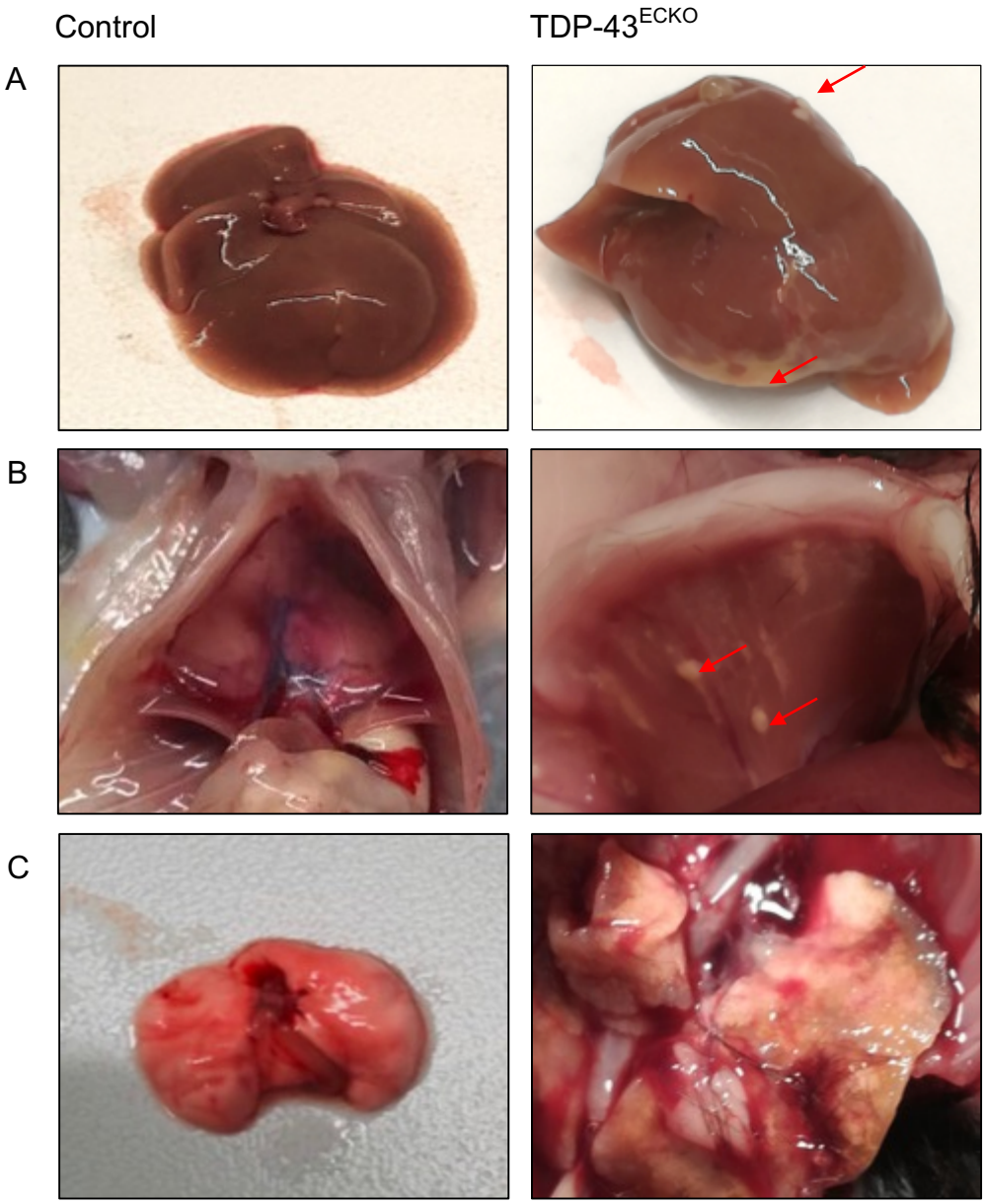

Figure 15. Changes in various organs of TDP-43^{ECKO}

Macroscopic abnormalities were observed in the liver (A), the diaphragm (B) and lung (C) of TDP-43^{ECKO} mice but not in control mice. The livers of TDP-43^{ECKO} mice showed nodular structures and streaks at the edge and white "nodules" on its surface marked by arrows (A). Some diaphragms of TDP-43^{ECKO} mouse also showed these white "nodules" marked by arrows (B). Lungs of TDP-43^{ECKO} mice already lost their normal structure compared with control mice (C).

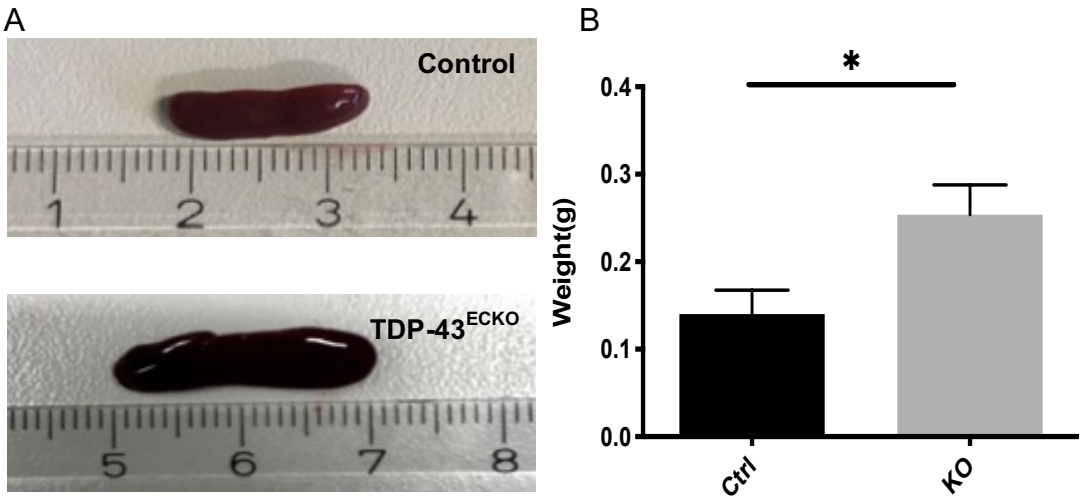

Figure 16. Increased spleen size in TDP-43^{ECKO} mice compared to control mice

Spleen size of TDP-43^{ECKO} mice was enlarged compared to control mice (A). Spleen weight was also significantly increased in TDP-43^{ECKO} mice compared to control mice (B). (control mice n=3, TDP-43^{ECKO} mice n=5, mean ± SEM, * $p<0.05$. unpaired t-test;)

3.3.2 EC-specific deletion of TDP-43 results in perivascular infiltration of lymphocytes

Histopathological analysis of the liver was carried out, and we observed surprisingly a massive infiltration of round-shaped cells around hepatic vessels of TDP-43^{ECKO} mice, which was absent in the liver tissue from control mice (Figure 17). Further analysis showed that the observed perivascular infiltration of cells was not only present in the liver, but also detectable in the kidney and lung tissue of mice lacking EC TDP-43. We characterized these cells by immunohistochemistry as lymphocytes (see below). Moreover, the "nodules" located on the surface of diaphragm from TDP-43^{ECKO} mice could also be defined as a collection of lymphocytes.

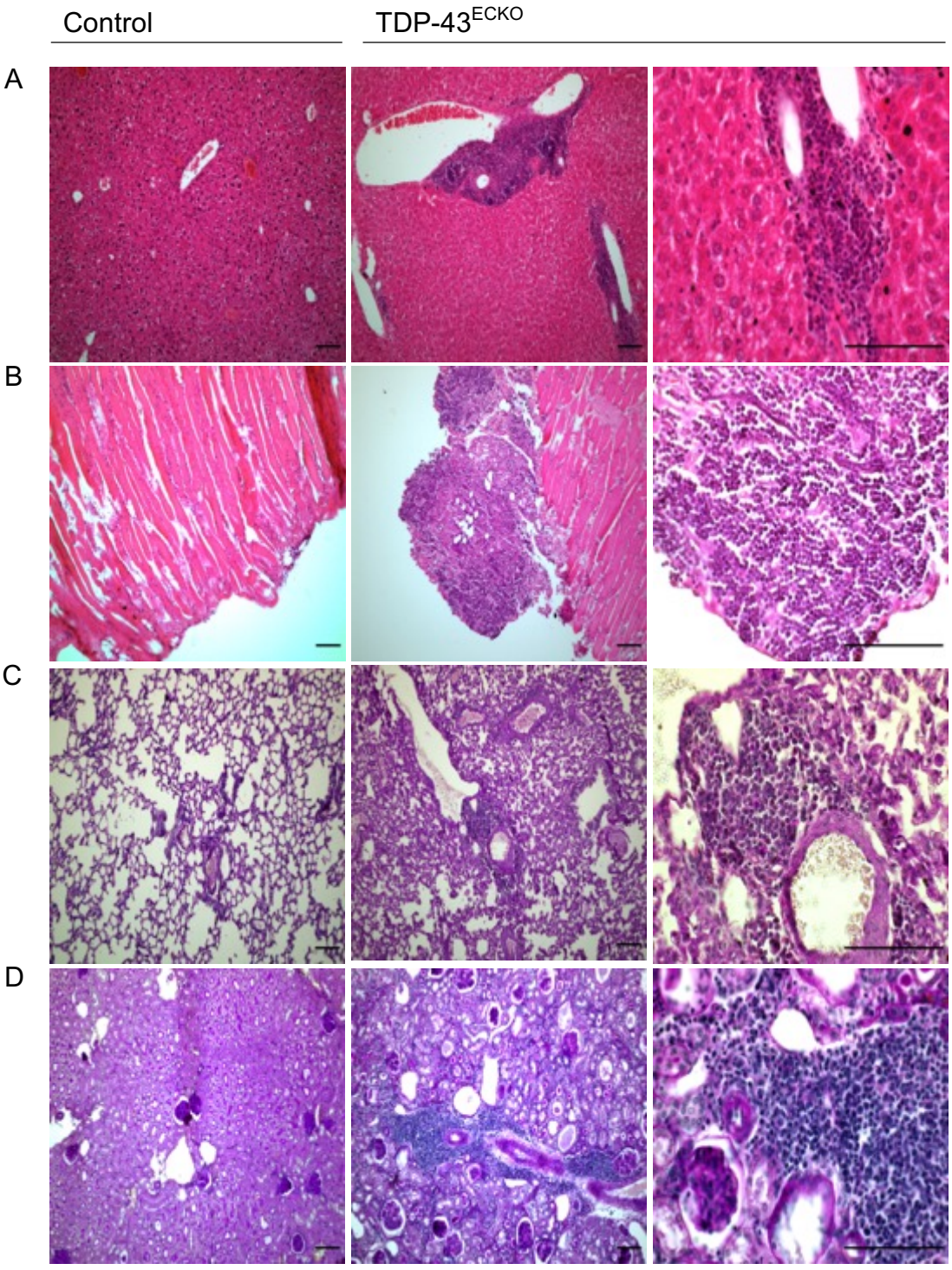

Figure 17. TDP-43 deficiency in EC leads to lymphocyte infiltration

H&E staining of livers (A), diaphragms (B) and PAS staining of lungs (C) and kidneys (D). Perivascular infiltration of round-shaped cells was observed in the liver (A), lung (C) and kidney (D) of TDP-43^{ECKO} mice but not in control mice. The white nodules on the surface of diaphragms of TDP-43^{ECKO} mice also demonstrated accumulation of round shaped cells (C). Scale bar=100 μm.

3.3.3 Both, B-lymphocytes and T-lymphocytes contribute to perivascular lymphocyte infiltration in the liver tissue.

In order to investigate which type of cells infiltrated into the tissues, we performed immunohistochemistry. Interestingly, most of the cells could be defined as lymphocytes. As displayed in Figure 18 both, B-lymphocytes and T-lymphocytes were the main extravasated cells around the vessels in the liver of TDP-43^{ECKO} mice.

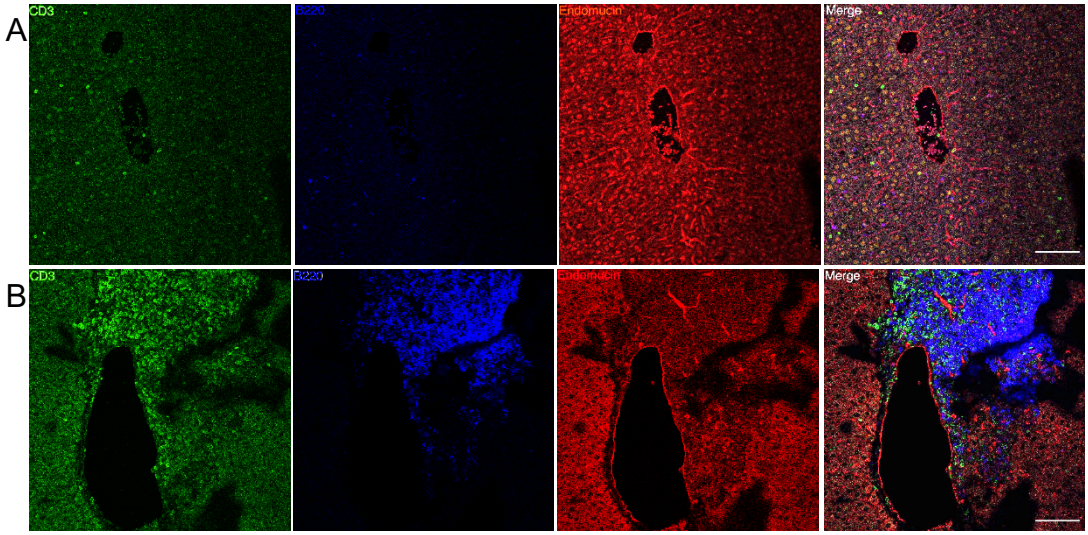

Figure 18. Fluorescence microscopy of liver sections

Immunofluorescence staining for EC marker Endomucin (red color), B-lymphocyte marker CD45R (blue color) and T lymphocyte marker CD3 (green color), revealed a massive infiltration of lymphocytes in the hepatic tissue. Both, B-lymphocytes (blue color) as well as T-lymphocytes (green color) infiltrated tissues around the hepatic vessel of TDP-43^{ECKO} mice (B) which was not observed in control mice (A). scale bar=100 µm.

3.4 Lymphocyte accumulation increased in the liver of TDP-43^{ECKO} mice

In order to quantify the number of infiltrated lymphocytes, flow cytometry analysis was performed using different organs. By use of anti-CD45R and anti-CD3 antibodies, B cells and T cells could be identified. As shown in the Figure 19, both, B cell and T cells were significantly increased in the liver of TDP-

43^{ECKO} mice compared to TDP-43^{Ctrl} mice. For the lung, kidney and spleen, there were no difference in both, B and T cells between the two groups.

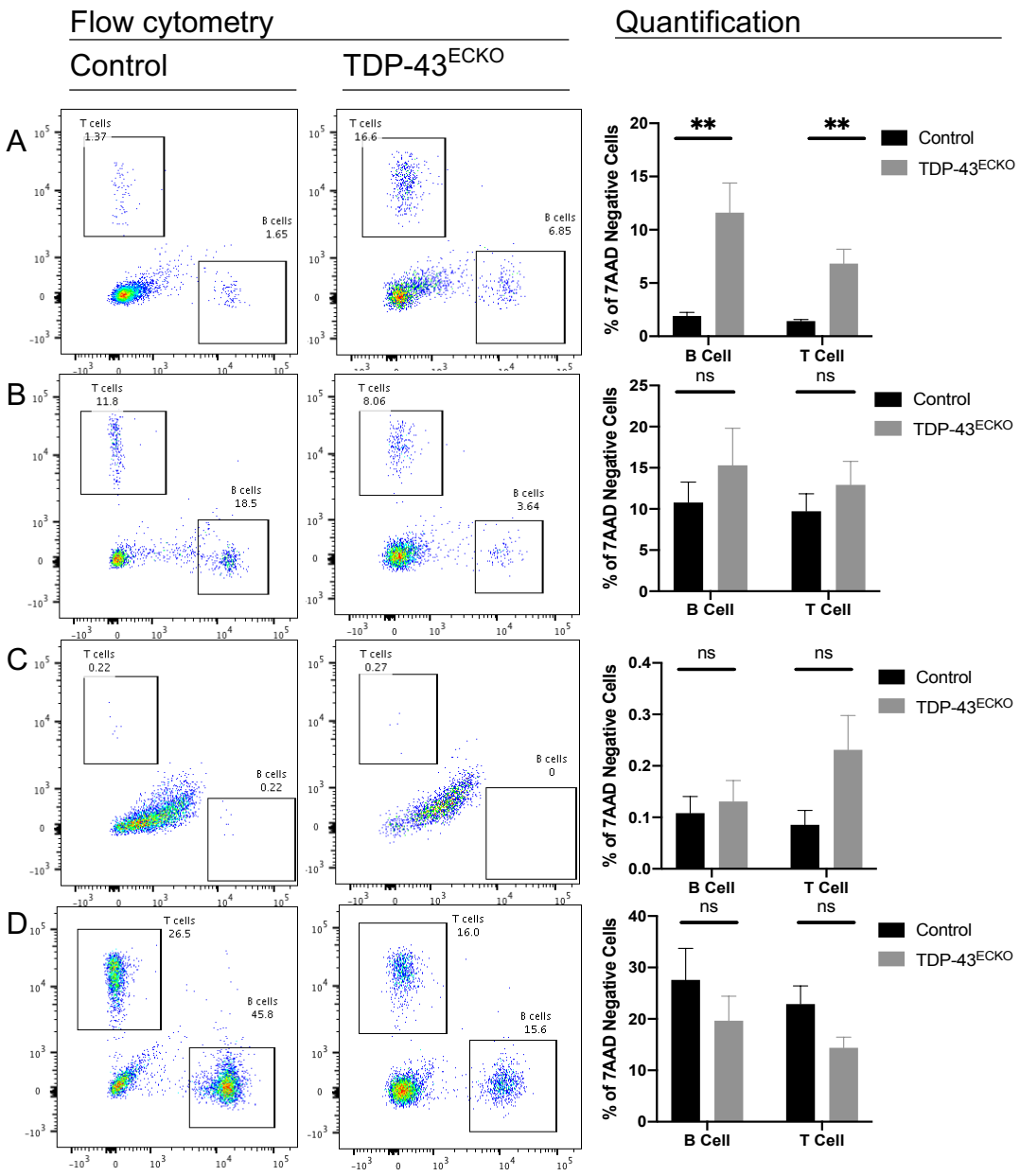

Figure 19. Lymphocyte populations in different organs

Organs were harvested and analyzed by flow cytometry. Gating of B cell and T cell populations in the liver (A), lung (B), kidney (C) and spleen (D) of mice. Both, B cell and T cell populations increased significantly in the liver tissue of TDP-43^{ECKO} mice compared to control mice. (n=8-11 per group, mean ± SEM, ns: not significant, ** p<0.01, t-test)

3.5 EC-specific deletion of TDP-43 and leukocyte recruitment

In order to study the potential role of TDP-43 in leukocyte recruitment in *vivo*, intravital microscopy was applied in the mouse cremaster muscle. EC-specific deletion of TDP-43 in adult mice did not influence leukocyte rolling flux fraction, but resulted in an increase in the number of adherent leukocytes compared to control mice. Moreover, leukocyte rolling velocity was reduced significantly in TDP-43^{ECKO} mice compared to control mice (Figure 20).

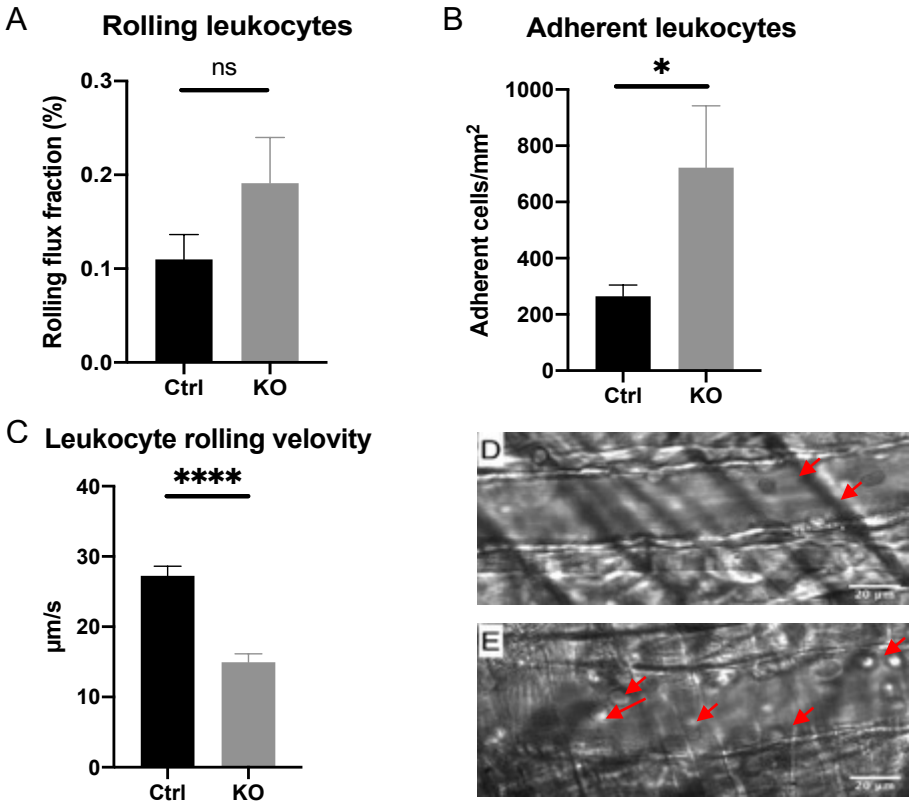

Figure 20. EC-specific deletion of TDP-43 increases leukocyte adhesion and decreases rolling velocity in *vivo*

Intravital microscopy of post-capillary venules in the cremaster muscle was carried out. Rolling flux fraction (A) and adherent leukocytes (B) were analyzed in 12 venules of 3 control mice and 9 venules of 3 TDP-43^{ECKO} mice. Leukocyte rolling velocity (C) was analyzed in 111 cells of 3 control and 55 cells of 2 TDP-43^{ECKO} mice. Representative micrographs of both control and TDP-43^{ECKO} mice are shown respectively (D and E). Leukocytes are marked by arrows. (n=3 mice, mean ± SEM, ns: not significant, * $p<0.05$, **** $p<0.0001$, t-test)

3.6 Knockdown of TDP-43 by siRNA in HUVECs promotes lymphocyte adhesion induced by TNF-α in *vitro*

In order to investigate the potential impact of endothelial-cell specific deletion of TDP-43 on lymphocyte recruitment, in *vitro* flow chamber assays were performed. HUVECs were cultured and transfected by siRNA in ibidi chambers to down-regulate TDP-43 expression in HUVECs. Immunofluorescence staining was performed to check TDP-43 knockdown efficiency. As shown in Figure 21, the expression level of TDP-43 in HUVECs transfected with TDP-43 siRNA was clearly decreased compared to HUVECs transfected with control siRNA.

Flow chamber assays were performed 3 days after siRNA treatment. HUVECs were pretreated with or without human TNF-α (10ng/ml) for 4 hours. Afterwards, the chambers were perfused with lymphocytes isolated from human blood. Interestingly, in HUVECs coated chambers without human TNF-α treatment, no rolling and adherent lymphocytes could be observed. However, a significant increase in the number of adherent lymphocytes was observed after treatment with human TNF-α. Interestingly, downregulation of TDP-43 in HUVECs further promotes lymphocyte adhesion induced by human TNF-α (Figure 22), suggesting that TDP-43 negatively regulates lymphocyte recruitment.

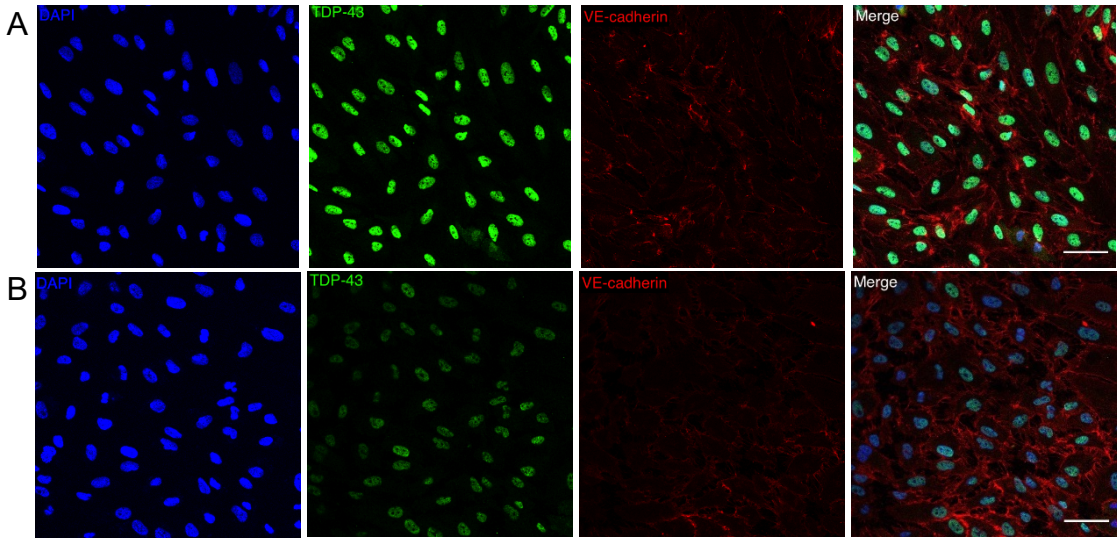

Figure 21. Decreased expression of TDP-43 in TDP-43 siRNA treated HUVECs

In order to check the TDP-43 Knock-down efficiency in HUVECs, IF staining was carried out. TDP-43 expression (green color) of KD HUVECs (B) was clearly decreased compared to control HUVECs (A). Scale bar=50μm, blue: DAPI, green: TDP-43, red: VE-cadherin.

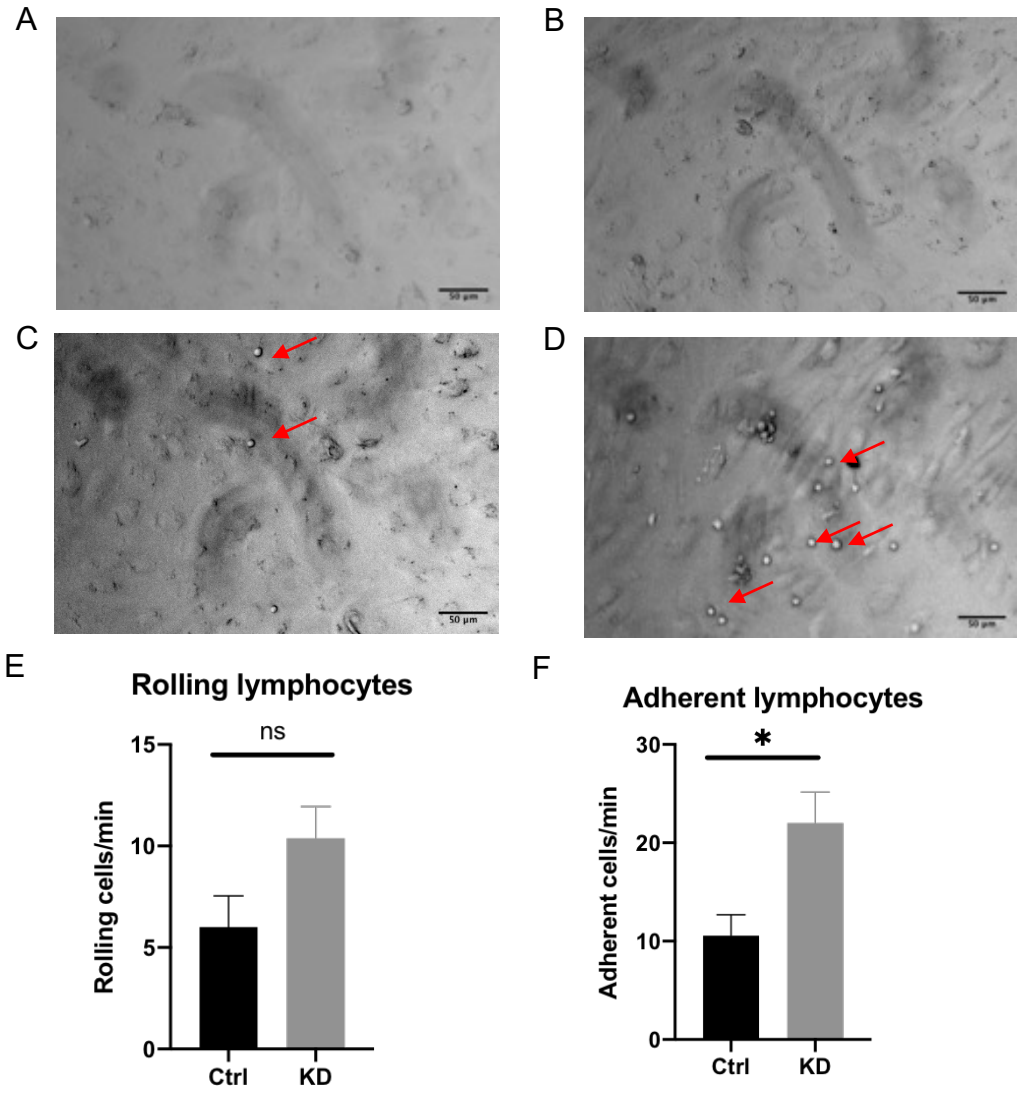

Figure 22. Knockdown of TDP-43 in HUVECs facilitates lymphocyte adhesion

Representative micrographs are shown. (A) HUVECs transfected with control siRNA and (B) HUVECs transfected with TDP-43 siRNA showed no rolling and no adherent lymphocytes on the surface of HUVECs without stimulation. Figure C and D show that treatment of HUVECs with human TNF-α induced adherence and rolling of lymphocytes (arrows). Rolling lymphocytes (E) and adherent lymphocytes (F) were quantified in micro flow chambers coated with HUVECs. Adherent lymphocytes but not rolling lymphocytes increased significantly in the KD group compared to the control group (E and F) (n=7/8, mean ± SEM, *: ≤0.05, ns not significant, Mann Whitney Rank Sum test)

3.7 Fibronectin expression following TDP-43 silencing in HUVECs

As KD of TDP-43 in HUVECs facilitated lymphocyte adhesion induced by TNF-α, we aimed to investigate whether the KD of TDP-43 is able to induce upregulation of adhesion and cellular matrix molecules on HUVECs in *vitro*. HUVECs were cultured and transfected with control siRNA or siRNA designed to silence the expression of TDP-43. After three days of transfection, HUVECs were harvested and immunoblotting was carried out. The expression level of TDP-43 was significantly decreased in the cells transfected with TDP-43 siRNA compared to control HUVECs (Figure 23A, B). Furthermore, the expression level of fibronectin was significantly increased in TDP-43 siRNA transfected HUVECs compared with control siRNA cells (Figure 23A, C). We also tested whether the KD of TDP-43 increased VCAM-1 expression. However, we could not detect any VCAM-1 expression by western blot in both groups.

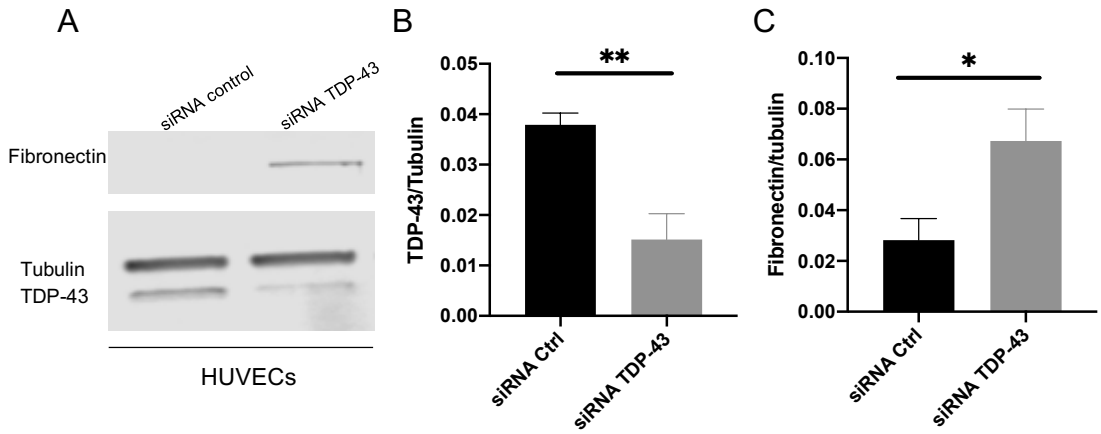

Figure 23. Decreased expression of TDP-43 leads to upregulation of fibronectin

A representative western blot is shown for analysis of TDP-43 and fibronectin expression in cell lysates from HUVECs transfected with control siRNA and TDP-43 siRNA (A). Expression of TDP-43 in TDP-43 siRNA treated HUVECs was significantly decreased compared with control cells (B). Expression of fibronectin in TDP-43 siRNA treated HUVECs was significantly higher than in control cells (C). (n=3, mean ± SEM, * $p<0.05$, ** <0.01, t-test)

3.8 Mice with EC-specific deletion of TDP-43 suffer from anemia, thrombocytopenia and lymphopenia

In order to assess whether EC loss of TDP-43 leads to changes of blood cell parameters, blood was collected and cell numbers counted using Procyte DXcell counter with mouse hematology settings. TDP-43^{ECKO} mice showed normochromic-normocytic anemia, which was accompanied by a significantly increased proportion of reticulocytes. In addition, thrombocytopenia and lymphopenia were observed in some TDP-43^{ECKO} mice (Figure 24).

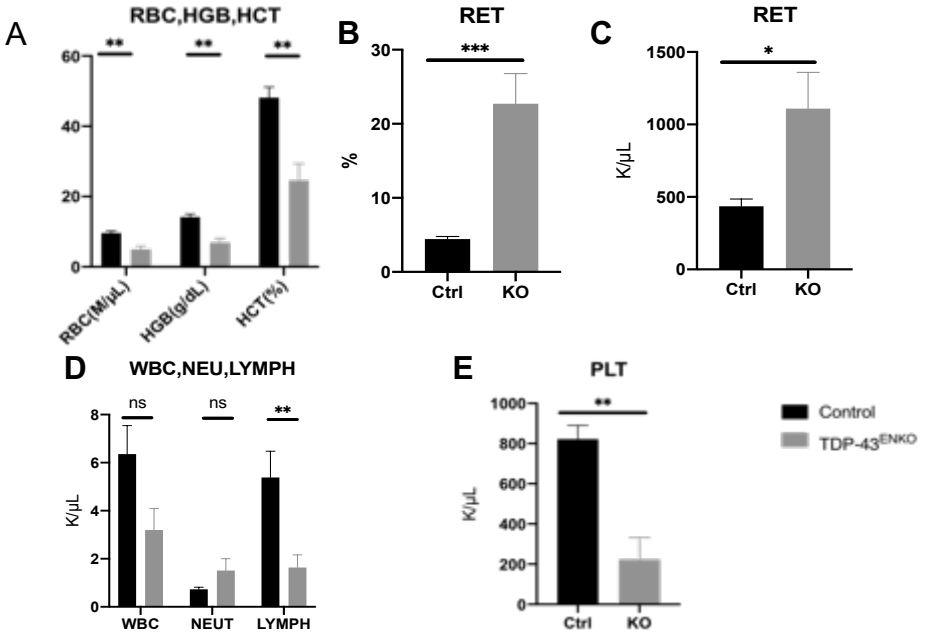

Figure 24. Total blood cell count

Total blood cells were measured by Procyte DXcell counter and showed dramatic differences between TDP-43^{ECKO} and control mice. RBC, HGB and HCT were significantly decreased in TDP-43^{ECKO} mice compared to control mice (n=7, mean ± SEM, ** $p<0.01$, Mann Whitney Rank Sum test) (A). An opposite trend was observed in RET (n=7, mean ± SEM, * $p<0.05$, *** $p<0.001$, t test) (B, C). The number of WBC did not show any differences between the groups, but the number of lymphocytes decreased significantly in TDP-43^{ECKO} mice compared to control mice (n=7, mean ± SEM, ns: not significant, ** $p<0.01$, t test) (D). Moreover, the number of platelets also decreased significantly in TDP-43^{ECKO} mice (n=7, mean ± SEM, ** $p<0.01$, Mann Whitney Rank Sum test) (E).

4 Discussion

TDP-43 is a DNA/RNA binding protein that has multiple functions in gene regulation (Ou et al. 1995, Liu et al. 2010, Buratti et al. 2008). Dislocation and aggregation of TDP-43 in neuronal cells plays an important role in neurodegenerative diseases such as amyotrophic lateral sclerosis (ALS) and frontotemporal lobar degeneration (FTDL) (Neumann et al. 2006, Chen et al. 2010, Arai et al. 2006). Studies on TDP-43 mainly focused on neurodegenerative diseases (Chakravorty et al. 1999, Arai et al. 2006). However, Schmid et al reported that TDP-43 was involved in the development of blood vessels. Double mutants of TDP-43 ($tardbp^{-/-}$; $tardbpl^{-/-}$) zebrafish revealed a dramatic mispatterning of blood vessels in both head and trunk (Schmid et al. 2013).

As reported previously, complete loss of TDP-43 results in embryonic lethality in mice between day 3.5 and day 8.5 of embryonic development (Sephton et al. 2020, Wu et al. 2020, Kraemer et al. 2020). Since we aimed to investigate the function of TDP-43 in the vascular system of adult mice, an inducible mouse model was used. In detail, mice in which LoxP sites were inserted in exon 3 of tardbp were mated with mice that carry Cre recombinase activated by a tamoxifen-inducible endothelial cell specific promoter. In this way, EC specific deletion of TDP43 can be induced by administration of tamoxifen and the function of TDP-43 in the vascular system can be investigated in the mice.

Although an important role of TDP-43 has been described for the development of vasculature, little is known to which extent TDP-43 might play a role in the endothelial cell function after development. Therefore, the aim of this thesis was to investigate whether TPD-43 influences vascular function in adult mice.

The experimental work presented here unveiled that loss of TDP-43 in endothelial cells of mice does not have an impact on vasoconstriction and

vasodilation in an isolated femoral artery model, but induces massive perivascular infiltration of lymphocytes into different kinds of organs.

4.1 Arterial function in TDP-43^{ECKO} mice

Resistance arteries are involved in controlling peripheral vascular resistance (Luksha et al. 2011). Vascular endothelium plays a fundamental role in regulating vascular tone by synthesizing and releasing a number of vasoactive substances (Spieker et al. 2006, Lüscher et al. 1993, Sandoo et al. 2010). Dysfunction of endothelial cells impacts vascular tone and in turn may lead to hypertension (Sandoo et al. 2010).

TDP-43 is a nuclear protein and transcriptional repressor that can modulate gene expression (Ou et al. 1995, Liu et al. 2010, Buratti et al. 2008). Loss of TDP-43 in zebrafish caused substantial defects of the vascular system (Schmid et al. 2013). Therefore, we first investigated whether the EC-specific loss of TDP-43 in adult mice also plays an import role in the regulation of the vascular tone. Isolated femoral arteries, which were used in many studies to investigate endothelium-dependent dilation of arteries (Bolz et al. 1999, Schneider et al .2015), were used in this thesis to investigate vasomotor function. We did not observe any differences in vasodilation and vasoconstriction function of femoral arteries in adult mice with or without EC-specific deletion of TDP-43.

In addition to vasomotor function, the original diameters of femoral arteries were also measured immediately after isolation under 60 mmHg. No differences between TDP-43^{ECKO} and control mice could be recorded.

Therefore, we conclude that TDP-43 expression in endothelial cells does not have an impact on vascular tone and vasoreactivity of femoral arteries of adult mice.

4.2 Perivascular infiltration of lymphocytes

We detected conspicuous general findings in many organs of TDP-43^{ECKO} mice. These changes differed in severity between individual mice. For example, we found a massive perivascular infiltration of lymphocytes into the liver tissue of EC-specific TDP-43 knockout mice. Normally, lymphocytes are found in sinusoids of normal liver and play their role in protecting against viral infections or sterile inflammation (Shetty et al. 2008, Racanelli et al. 2006, Selmi et al. 2007, Doherty et al. 2000). Location of lymphocyte infiltration into the liver depends on the inflammatory stimulus. Infiltration of lymphocytes to portal tracts may indicate biliary disease or acute allograft rejection in transplanted patients (Borchers et al. 2009, Shi et al. 2017). Infiltration into the parenchyma is a symbol of acute viral hepatitis or autoimmune hepatitis (Lalor et al. 2002). Transgenic mice carrying hepatitis C virus revealed recruitment of T lymphocytes into the liver where lymphocytes mainly distributed in the parenchyma and occasionally around central-lobular or portal vessels (Alonzi et al. 2004). Here we show that loss of TDP-43 in the endothelium leads to lymphocyte accumulation around blood vessels of the liver, but not portal tracts and parenchyma. This could indicate that EC-specific deletion of TDP-43 leads to a change in the protein expression pattern of ECs thereby triggering perivascular infiltration of lymphocytes. Such phenomenon was also observed in the kidney and lung tissues. Indeed, by binding both, DNA and RNA, TDP-43 can regulate gene expression which in turn can influence the expression of proteins (Ou et al. 1995, Liu et al. 2010, Buratti et al. 2008). Therefore, we speculate that deletion of TDP-43 in EC may regulate expression of selectins which results in perivascular infiltration of lymphocytes in the tissues.

Furthermore, blood examination was performed and revealed that TDP-43^{ECKO} mice showed a normochromic and normocytic anemia with a significantly increased proportion of reticulocytes. In line, we often detected an enlarged spleen which might indicate that a large number of red blood cells maybe destroyed in the spleen. However, we also observed bleedings in some of the organs which also could explain anemia and high numbers of reticulocytes.

Ongoing studies using Prussian Blue staining demonstrated no increase in amounts of ferric iron in spleen tissue derived from TDP-43^{ECKO} mice so far. Moreover, lymphopenia was also observed in the TDP-43^{ECKO} mice, but not in control mice. This phenomenon may be caused by the recruitment of a large number of lymphocytes into the organs.

4.3 TDP-43 in endothelial cells regulates leukocyte recruitment in *vivo*

Both innate and adaptive immune responses are important for the host defense against foreign challenges (Luster et al. 2002). Neutrophils are a critical component of the innate immune response, whereas adaptive immune responses are mediated by lymphocytes (Massberg et al. 2010, Hawkins et al. 2013). In response to inflammation, leukocytes exit the vasculature from the blood circulation into inflamed tissues through a cascade of adhesion activation steps starting with tethering and rolling of leukocytes along endothelial cells (Ley et al. 2007). During this process, endothelial cells play an important role in regulating leukocyte recruitment to inflamed tissues. They are activated by inflammation and express various adhesion molecules that mediate leukocytes and endothelial cell interaction (Ley et al. 2007).

Using intravital microscopy to study inflamed cremaster muscle, leukocyte rolling, adhesion and rolling velocity, as well as hemodynamic parameters such as vessel diameter, vessel length and blood flow velocity were analyzed (Kurz et al. 2016, Rohwedder et al. 2020). Loss of TDP-43 in ECs did not impact leukocyte rolling, but facilitates leukocyte adhesion. Leukocyte adhesion during rolling is mediated by the interaction of leukocyte integrins with various adhesion molecules expressed by endothelial cells such as ICAM-1 and VCAM-1 (Barreiro et al. 2003, Diamond et al.1991). TDP-43 is a nuclear protein that binds both, DNA and RNA and has multiple functions in the regulation of gene expression (Ou et al. 1995, Buratti et al. 2008, Liu et al. 2010). Therefore, we deduce that KO of TDP-43 in ECs may affect the expression of adhesion molecules that in return facilitate leukocyte adhesion. From our cremaster

model experiment, we can conclude that TDP-43 expression in endothelial cells is involved in leukocyte adhesion, but we cannot confirm whether these leukocytes are mainly lymphocytes. Therefore, further experiments are necessary to study the involvement of loss of TDP-43 expression in endothelial cells in leukocyte/lymphocyte recruitment to the inflamed cremaster muscle similar to what could be observed in the liver of TDP-43^{ECKO} mice.

4.4 Flow chamber experiments

HUVECs are cells isolated from veins of the umbilical cord. They are usually used as a laboratory model system for the investigation of the regulation of EC function and the role of ECs in the development of inflammation, atherosclerosis and angiogenesis (Medina-Leyte et al. 2020, Chen et al .2013). In our microflow chamber assay, HUVECs were utilized for the analysis of how TDP-43 regulates the interaction of lymphocytes with HUVECs.

In our mouse model, we observed a massive perivascular infiltration of lymphocytes in liver tissue. So, we first aimed to analyze if the loss of TDP-43 in HUVECs alone could induce interaction of lymphocytes with HUVECs in *vitro*. For this purpose, a lymphocyte suspension was directly perfused under a constant flow rate through the microflow chamber without any treatment of HUVECs. However, no interaction of lymphocytes with HUVECs could be observed in both, TDP-43 siRNA-treated HUVECs and the control group, which indicates that the downregulation of TDP-43 alone does not affect lymphocyte recruitment in *vitro*.

Inflammation of HUVECs can be induced by hTNF-α treatment (Liu et al. ,2019). So, in order to investigate whether TDP-43 expression can influence the interaction of lymphocytes with inflamed HUVECs, HUVECs were treated with hTNF-α to induce inflammation. Compared to control HUVECs, reduction of TDP-43 in HUVECs did not influence lymphocyte rolling, but facilitates lymphocyte adhesion induced by hTNF-α. Lymphocyte adhesion is mediated by the interaction of VCAM-1 and ICAM-1 with VLA-4 and LFA-1, respectively

(Chakravorty et al. 1999, Dianzani et al. 1995). After treatment with TNF-α, HUVECs express adhesion molecules such as VCAM-1, ICAM-1 and E-selectin that mediate the interaction between lymphocytes and endothelial cells (Chakravorty et al. 1999, Dianzani et al. 1995, Leeuwenberg et al. 1992, Zhou et al. 2005). Therefore, we speculate that TDP-43 knock-down can regulate lymphocyte adhesion to inflamed HUVECs, but not to normal HUVECs in *vitro*. The differences between the in *vitro* and in *vivo* experiments might be related to the different levels of TDP-43 expression (knockdown by siRNA versus genetic deletion).

4.6 Outlook

TDP-43 has been well investigated in neurodegenerative disorders, but no study has focused on its role in lymphocyte recruitment. We discovered that loss of TDP-43 expression in endothelial cells results in massive perivascular infiltration of both, T and B lymphocytes into different organs. The perivascular infiltration of lymphocytes was most prominent in the liver, but also appeared in the kidney and lung in several EC-specific TDP-43 knockout mice. On the opposite, we speculate that under normal conditions, TDP-43 expression in the endothelium is an important factor that blocks T- and B-lymphocyte infiltration in tissues. Further research may focus on the exact molecular mechanisms that lead to infiltration of lymphocytes in different organs.

Furthermore, in our in *vivo* and in *vitro* experiments, we found that TDP-43 plays a potential role in regulating lymphocyte migration. Although the lower level of TDP-43 in HUVECs increased the expression of fibronectin which may be involved in this process in *vitro*, the mechanisms of how TDP-43 plays its role in regulating lymphocyte migration are still unknown. Thus, this study provides the basis for future investigations how TDP-43 in ECs regulates lymphocyte recruitment.

References

Ou, S. H., Wu, F., Harrich, D., García-Martínez, L. F., & Gaynor, R. B. (1995). Cloning and characterization of a novel cellular protein, TDP-43, that binds to human immunodeficiency virus type 1 TAR DNA sequence motifs. *Journal of virology*, *69*(6), 3584-3596.

Buratti, E., & Baralle, F. E. (2008). Multiple roles of TDP-43 in gene expression, splicing regulation, and human disease. Front Biosci, 13(867-7), 8.

Liu-Yesucevitz, L., Bilgutay, A., Zhang, Y. J., Vanderwyde, T., Citro, A., Mehta, T., ... & Petrucelli, L. (2010). Tar DNA binding protein-43 (TDP-43) associates with stress granules: analysis of cultured cells and pathological brain tissue. *PloS one*, *5*(10), e13250.

Neumann, M., Sampathu, D. M., Kwong, L. K., Truax, A. C., Micsenyi, M. C., Chou, T. T., ... & McCluskey, L. F. (2006). Ubiquitinated TDP-43 in frontotemporal lobar degeneration and amyotrophic lateral sclerosis. *Science*, *314*(5796), 130-133.

Schmid, B., Hruscha, A., Hogl, S., Banzhaf-Strathmann, J., Strecker, K., van der Zee, J., ... & Kremmer, E. (2013). Loss of ALS-associated TDP-43 in zebrafish causes muscle degeneration, vascular dysfunction, and reduced motor neuron axon outgrowth. *Proceedings of the National Academy of Sciences*, *110*(13), 4986-4991.

Gendron, T. F., Josephs, K. A., & Petrucelli, L. (2010). transactive response DNA-binding protein 43 (TDP-43): mechanisms of neurodegeneration. *Neuropathology and applied neurobiology*, *36*(2), 97-112.

Buratti, E., Dörk, T., Zuccato, E., Pagani, F., Romano, M., & Baralle, F. E. (2001). Nuclear factor TDP-43 and SR proteins promote in *vitro* and in *vivo* CFTR exon 9 skipping. *The EMBO journal*, *20*(7), 1774-1784.

Delaney, S. J., Rich, D. P., Thomson, S. A., Hargrave, M. R., Lovelock, P. K., Welsh, M. J., & Wainwright, B. J. (1993). Cystic fibrosis transmembrane conductance regulator splice variants are not conserved and fail to produce chloride channels. *Nature genetics*, *4*(4), 426-430.

Buratti, E., & Baralle, F. E. (2001). Characterization and Functional Implications of the RNA Binding Properties of Nuclear Factor TDP-43, a Novel Splicing Regulator ofCFTR Exon 9. *Journal of Biological Chemistry*, *276*(39), 36337-36343.

Arai, T., Hasegawa, M., Akiyama, H., Ikeda, K., Nonaka, T., Mori, H., ... & Oda, T. (2006). TDP-43 is a component of ubiquitin-positive tau-negative inclusions in frontotemporal lobar degeneration and amyotrophic lateral sclerosis. *Biochemical and biophysical research communications*, *351*(3), 602-611.

Chen-Plotkin, A. S., Lee, V. M. Y., & Trojanowski, J. Q. (2010). TAR DNA-binding protein 43 in neurodegenerative disease. *Nature Reviews Neurology*, *6*(4), 211-220.

Zhang, Y. J., Xu, Y. F., Cook, C., Gendron, T. F., Roettges, P., Link, C. D., ... & Gass, J. (2009). Aberrant cleavage of TDP-43 enhances aggregation and cellular toxicity. *Proceedings of the National Academy of Sciences*, *106*(18), 7607-7612.

Sato, Y. (2001). Current understanding of the biology of vascular endothelium. *Cell Structure and Function*, *26*(1), 9-10.

Ghitescu, L., & Robert, M. (2002). Diversity in unity: the biochemical composition of the endothelial cell surface varies between the vascular beds. *Microscopy research and technique*, *57*(5), 381-389.

Mehta, D., & Malik, A. B. (2006). Signaling mechanisms regulating endothelial permeability. *Physiological reviews*.

Sandoo, A., van Zanten, J. J. V., Metsios, G. S., Carroll, D., & Kitas, G. D. (2010). The endothelium and its role in regulating vascular tone. *The open cardiovascular medicine journal*, *4*, 302.

Pober, J. S., & Sessa, W. C. (2007). Evolving functions of endothelial cells in inflammation. *Nature Reviews Immunology*, *7*(10), 803-815.

Ferrara, N. (2000). Vascular endothelial growth factor and the regulation of angiogenesis. *Recent progress in hormone research*, *55*, 15.

Vallance, P., Collier, J., & Moncada, S. (1989). Effects of endothelium-derived nitric oxide on peripheral arteriolar tone in man. *The Lancet*, *334*(8670), 997-1000.

Lüscher, T. F., & Tanner, F. C. (1993). Endothelial regulation of vascular tone and growth. *American journal of hypertension*, *6*(7_Pt_2), 283S-293S.

Palmer, R. M., Ashton, D. S., & Moncada, S. (1988). Vascular endothelial cells synthesize nitric oxide from L-arginine. *Nature*, *333*(6174), 664-666.

Bucci, M., Gratton, J. P., Rudic, R. D., Acevedo, L., Roviezzo, F., Cirino, G., & Sessa, W. C. (2000). In *vivo* delivery of the caveolin-1 scaffolding domain inhibits nitric oxide synthesis and reduces inflammation. *Nature medicine*, *6*(12), 1362-1367.

Butt, E., Bernhardt, M., Smolenski, A., Kotsonis, P., Fröhlich, L. G., Sickmann, A., ... & Schmidt, H. H. (2000). Endothelial nitric-oxide synthase (type III) is activated and becomes calcium independent upon phosphorylation by cyclic nucleotide-dependent protein kinases. *Journal of Biological Chemistry*, *275*(7), 5179-5187.

Boo, Y. C., Sorescu, G., Boyd, N., Shiojima, I., Walsh, K., Du, J., & Jo, H. (2002). Shear stress stimulates phosphorylation of endothelial nitric-oxide synthase at Ser1179 by Akt-independent mechanisms role of protein kinase A. *Journal of Biological Chemistry*, *277*(5), 3388-3396.

Derbyshire, E. R., & Marletta, M. A. (2009). Biochemistry of soluble guanylate cyclase. In *cGMP: Generators, Effectors and Therapeutic Implications* (pp. 17-31). Springer, Berlin, Heidelberg.

Yang, J., Clark, J. W., Bryan, R. M., & Robertson, C. S. (2005). Mathematical modeling of the nitric oxide/cGMP pathway in the vascular smooth muscle cell. *American Journal of Physiology-Heart and Circulatory Physiology*, *289*(2), H886-H897.

Spier, S. A., Delp, M. D., Stallone, J. N., Dominguez, J. M., & Muller-Delp, J. M. (2007). Exercise training enhances flow-induced vasodilation in skeletal muscle resistance arteries of aged rats: role of PGI2 and nitric oxide. American Journal of Physiology-Heart and Circulatory Physiology, 292(6), H3119-H3127.

Clapp, L. H., Finney, P., Turcato, S., Tran, S., Rubin, L. J., & Tinker, A. (2002). Differential effects of stable prostacyclin analogs on smooth muscle proliferation and cyclic AMP generation in human pulmonary

artery. *American journal of respiratory cell and molecular biology*, *26*(2), 194-201.

Fetalvero, K. M., Martin, K. A., & Hwa, J. (2007). Cardioprotective prostacyclin signaling in vascular smooth muscle. *Prostaglandins & other lipid mediators*, *82*(1-4), 109-118.

Kamm, K. E., & Stull, J. T. (1985). The function of myosin and myosin light chain kinase phosphorylation in smooth muscle. *Annual review of pharmacology and toxicology*, *25*(1), 593-620.

Goeckeler, Z. M., Masaracchia, R. A., Zeng, Q., Chew, T. L., Gallagher, P., & Wysolmerski, R. B. (2000). Phosphorylation of myosin light chain kinase by p21-activated kinase PAK2. *Journal of Biological Chemistry*, *275*(24), 18366-18374.

Vestweber, D. (2015). How leukocytes cross the vascular endothelium. *Nature Reviews Immunology*, *15*(11), 692-704.

Schmidt, S., Moser, M., & Sperandio, M. (2013). The molecular basis of leukocyte recruitment and its deficiencies. Molecular immunology, 55(1), 49-58.

McEver, R. P. (2015). Selectins: initiators of leucocyte adhesion and signalling at the vascular wall. *Cardiovascular research*, *107*(3), 331-339.

Ley, K., Laudanna, C., Cybulsky, M. I., & Nourshargh, S. (2007). Getting to the site of inflammation: the leukocyte adhesion cascade updated. *Nature Reviews Immunology*, *7*(9), 678-689.

Kurz, A. R., Pruenster, M., Rohwedder, I., Ramadass, M., Schäfer, K., Harrison, U., Gouveia, G., Nussbaum, C., Immler, R., Wiessner, J. R., Margraf, A., Lim, D. S., Walzog, B., Dietzel, S., Moser, M., Klein, C., Vestweber, D., Haas, R., Catz, S. D., & Sperandio, M. (2016). MST1-dependent vesicle trafficking regulates neutrophil transmigration through the vascular basement membrane. The Journal of clinical investigation, 126(11), 4125–4139.

Rohwedder, I., Kurz, A., Pruenster, M., Immler, R., Pick, R., Eggersmann, T., Klapproth, S., Johnson, J. L., Alsina, S. M., Lowell, C. A., Mócsai, A., Catz, S. D., & Sperandio, M. (2020). Src family kinase-mediated vesicle

trafficking is critical for neutrophil basement membrane penetration. Haematologica, 105(7), 1845–1856.

da Costa Martins, P., García-Vallejo, J. J., van Thienen, J. V., Fernandez-Borja, M., van Gils, J. M., Beckers, C., ... & Zwaginga, J. J. (2007). P-selectin glycoprotein ligand-1 is expressed on endothelial cells and mediates monocyte adhesion to activated endothelium. *Arteriosclerosis, thrombosis, and vascular biology*, *27*(5), 1023-1029.

Campbell, J. J., Qin, S., Bacon, K. B., Mackay, C. R., & Butcher, E. C. (1996). Biology of chemokine and classical chemoattractant receptors: differential requirements for adhesion-triggering versus chemotactic responses in lymphoid cells. *Journal of Cell Biology*, *134*(1), 255-266.

Phillipson, M., Heit, B., Colarusso, P., Liu, L., Ballantyne, C. M., & Kubes, P. (2006). Intraluminal crawling of neutrophils to emigration sites: a molecularly distinct process from adhesion in the recruitment cascade. *The Journal of experimental medicine*, *203*(12), 2569-2575.

Barreiro, O., Yáñez-Mó, M., Serrador, J. M., Montoya, M. C., Vicente-Manzanares, M., Tejedor, R., ... & Sánchez-Madrid, F. (2002). Dynamic interaction of VCAM-1 and ICAM-1 with moesin and ezrin in a novel endothelial docking structure for adherent leukocytes. *The Journal of cell biology*, *157*(7), 1233-1245.

Shetty, S., Lalor, P. F., & Adams, D. H. (2008). Lymphocyte recruitment to the liver: molecular insights into the pathogenesis of liver injury and hepatitis. *Toxicology*, *254*(3), 136-146.

Racanelli, V., & Rehermann, B. (2006). The liver as an immunological organ. *Hepatology*, *43*(S1), S54-S62.

Shi, J., Gilbert, G. E., Kokubo, Y., & Ohashi, T. (2001). Role of the liver in regulating numbers of circulating neutrophils. Blood, The Journal of the American Society of Hematology, 98(4), 1226-1230.Braet, F., & Wisse, E. (2002). Structural and functional aspects of liver sinusoidal endothelial cell fenestrae: a review. *Comparative hepatology*, *1*(1), 1.

Steinhoff, G., Behrend, M., Schrader, B., Duijvestijn, A. M., & Wonigeit, K. (1993). Expression patterns of leukocyte adhesion ligand molecules on human liver endothelia. Lack of ELAM-1 and CD62 inducibility on

sinusoidal endothelia and distinct distribution of VCAM-1, ICAM-1, ICAM-2, and LFA-3. *The American journal of pathology*, *142*(2), 481.

Adams, D. H., Hubscher, S. G., Fisher, N. C., Williams, A., & Robinson, M. (1996). Expression of E-selectin and E-selectin ligands in human liver inflammation. *Hepatology*, *24*(3), 533-538.

Lalor, T., & Adams, D. (2002). The liver: a model of organ-specific lymphocyte recruitment. *Expert reviews in molecular medicine*, *4*(2), 1-15.

Edwards, S., Lalor, P. F., Nash, G. B., Rainger, G. E., & Adams, D. H. (2005). Lymphocyte traffic through sinusoidal endothelial cells is regulated by hepatocytes. *Hepatology*, *41*(3), 451-459.

Lalor, P. F., Edwards, S., McNab, G., Salmi, M., Jalkanen, S., & Adams, D. H. (2002). Vascular adhesion protein-1 mediates adhesion and transmigration of lymphocytes on human hepatic endothelial cells. *The Journal of Immunology*, *169*(2), 983-992.

Borchers, A. T., Shimoda, S., Bowlus, C., Keen, C. L., & Gershwin, M. E. (2009). Lymphocyte recruitment and homing to the liver in primary biliary cirrhosis and primary sclerosing cholangitis. Seminars in immunopathology, 31(3), 309–322.

Shi, Y., Dong, K., Zhang, Y. G., Michel, R. P., Marcus, V., Wang, Y. Y., Chen, Y., & Gao, Z. H. (2017). Sinusoidal endotheliitis as a histological parameter for diagnosing acute liver allograft rejection. World journal of gastroenterology, 23(5), 792–799.

Bonder, C. S., Norman, M. U., Swain, M. G., Zbytnuik, L. D., Yamanouchi, J., Santamaria, P., ... & Kubes, P. (2005). Rules of recruitment for Th1 and Th2 lymphocytes in inflamed liver: a role for alpha-4 integrin and vascular adhesion protein-1. *Immunity*, *23*(2), 153-163.

Lalor, P. F., Shields, P., Grant, A. J., & Adams, D. H. (2002). Recruitment of lymphocytes to the human liver. *Immunology and cell biology*, *80*(1), 52-64.

Lalor, P. F., & Adams, D. H. (1999). Adhesion of lymphocytes to hepatic endothelium. *Molecular Pathology*, *52*(4), 214.

Lipscomb, M. F., Lyons, C. R., O'Hara, R. M., & Stein-Streilein, J. (1982). The antigen-induced selective recruitment of specific T lymphocytes to the lung. *The Journal of Immunology*, *128*(1), 111-115.

BERNARDO, J., & CENTER, D. M. (1990). Lymphocyte Recruitment to the Lung1-3. *AM REV RESPIR DIS*, *142*, 238-257.

Aird, W. C. (2007). Phenotypic heterogeneity of the endothelium: II. Representative vascular beds. *Circulation research*, *100*(2), 174-190.

Randall, T. D. (2010). Bronchus-associated lymphoid tissue (BALT): structure and function. In *Advances in immunology* (Vol. 107, pp. 187-241). Academic Press.

Girard, J. P., & Springer, T. A. (1995). High endothelial venules (HEVs): specialized endothelium for lymphocyte migration. *Immunology today*, *16*(9), 449-457.

Xu, B., Wagner, N., Pham, L. N., Magno, V., Shan, Z., Butcher, E. C., & Michie, S. A. (2003). Lymphocyte homing to bronchus-associated lymphoid tissue (BALT) is mediated by L-selectin/PNAd, α4β1 integrin/VCAM-1, and LFA-1 adhesion pathways. *The Journal of experimental medicine*, *197*(10), 1255-1267.

Lipscomb, M. F., Lyons, C. R., O'Hara, R. M., & Stein Streilein, J. (1982). The antigen-induced selective recruitment of specific T lymphocytes to the lung. The Journal of Immunology,128(1), 111-115.

Bentley, A. M., Durham, S. R., Robinson, D. S., Menz, G., Storz, C., Cromwell, O., ... & Wardlaw, A. J. (1993). Expression of endothelial and leukocyte adhesion molecules intercellular adhesion molecule-1, E-selectin, and vascular cell adhesion molecule-1 in the bronchial mucosa in steady-state and allergen-induced asthma. *Journal of Allergy and Clinical Immunology*, *92*(6), 857-868.

Keramidaris, E., Merson, T. D., Steeber, D. A., Tedder, T. F., & Tang, M. L. (2001). L-selectin and intercellular adhesion molecule 1 mediate lymphocyte migration to the inflamed airway/lung during an allergic inflammatory response in an animal model of asthma. *Journal of allergy and clinical immunology*, *107*(4), 734-738.

Bohnsack, J. F., & Brown, E. J. (1986). The role of the spleen in resistance to infection. *Annual review of medicine*, *37*(1), 49-59.

Nolte, M. A., Hamann, A., Kraal, G., & Mebius, R. E. (2002). The strict regulation of lymphocyte migration to splenic white pulp does not involve common homing receptors. *Immunology*, *106*(3), 299-307.

Mebius, R. E., & Kraal, G. (2005). Structure and function of the spleen. *Nature reviews immunology*, *5*(8), 606-616.

Van Ewijk, W., & Nieuwenhuis, P. (1985). Compartments, domains and migration pathways of lymphoid cells in the splenic pulp. *Experientia*, *41*(2), 199-208.

Springer, T. A. (1994). Traffic signals for lymphocyte recirculation and leukocyte emigration: the multistep paradigm. *Cell*, *76*(2), 301-314.

Liu, Y., & Tie, L. (2019). Apolipoprotein M and sphingosine-1-phosphate complex alleviates TNF-α-induced endothelial cell injury and inflammation through PI3K/AKT signaling pathway. BMC Cardiovascular Disorders, 19(1), 279.

Chakravorty, S. J., Howie, A. J., Cockwell, P., Adu, D., & Savage, C. O. (1999). T lymphocyte adhesion mechanisms within inflamed human kidney: studies with a Stamper-Woodruff assay. *The American journal of pathology*, *154*(2), 503-514.

Chakravorty, S. J., Howie, A. J., Cockwell, P., Adu, D., & Savage, C. O. (1999). T lymphocyte adhesion mechanisms within inflamed human kidney: studies with a Stamper-Woodruff assay. *The American journal of pathology*, *154*(2), 503-514.

Luksha, N., Luksha, L., Carrero, J. J., Hammarqvist, F., Stenvinkel, P., & Kublickiene, K. (2011). Impaired resistance artery function in patients with end-stage renal disease. *Clinical Science*, *120*(12), 525-536.

Spieker, L. E., Flammer, A. J., & Lüscher, T. F. (2006). The vascular endothelium in hypertension. In *The Vascular Endothelium II* (pp. 249-283). Springer, Berlin, Heidelberg.

Lüscher, T. F., & Tanner, F. C. (1993). Endothelial regulation of vascular tone and growth. American journal of hypertension, 6(7 Pt 2), 283S–293S.

Bolz, S. S., De Wit, C., & Pohl, U. (1999). Endothelium-derived hyperpolarizing factor but not NO reduces smooth muscle Ca2+ during acetylcholine-induced dilation of microvessels. *British journal of pharmacology*, *128*(1), 124-134.

Schneider, H., Schubert, K. M., Blodow, S., Kreutz, C. P., Erdogmus, S., Wiedenmann, M., ... & Pfitzer, G. (2015). AMPK dilates resistance arteries via activation of SERCA and BKCa channels in smooth muscle. *Hypertension*, *66*(1), 108-116.

Sephton, C. F., Good, S. K., Atkin, S., Dewey, C. M., Mayer, P., Herz, J., & Yu, G. (2010). TDP-43 is a developmentally regulated protein essential for early embryonic development. *Journal of Biological Chemistry*, *285*(9), 6826-6834.

Wu, L. S., Cheng, W. C., Hou, S. C., Yan, Y. T., Jiang, S. T., & Shen, C. K. J. (2010). TDP-43, a neuro-pathosignature factor, is essential for early mouse embryogenesis. *genesis*, *48*(1), 56-62.

Kraemer, B. C., Schuck, T., Wheeler, J. M., Robinson, L. C., Trojanowski, J. Q., Lee, V. M., & Schellenberg, G. D. (2010). Loss of murine TDP-43 disrupts motor function and plays an essential role in embryogenesis. *Acta neuropathologica*, *119*(4), 409-419.

Selmi, C., Mackay, I. R., & Gershwin, M. E. (2007, August). The immunological milieu of the liver. In *Seminars in liver disease* (Vol. 27, No. 02, pp. 129-139). Copyright© 2007 by Thieme Medical Publishers, Inc., 333 Seventh Avenue, New York, NY 10001, USA..

Doherty, D. G., & O'Farrelly, C. (2000). Innate and adaptive lymphoid cells in the human liver. *Immunological reviews*, *174*(1), 5-20.

Luster, A. D. (2002). The role of chemokines in linking innate and adaptive immunity. *Current opinion in immunology*, *14*(1), 129-135.

Massberg, S., Grahl, L., von Bruehl, M. L., Manukyan, D., Pfeiler, S., Goosmann, C., ... & Konrad, I. (2010). Reciprocal coupling of coagulation and innate immunity via neutrophil serine proteases. *Nature medicine*, *16*(8), 887-896.

Hawkins, E. D., Turner, M. L., Wellard, C. J., Zhou, J. H. S., Dowling, M. R., & Hodgkin, P. D. (2013). Quantal and graded stimulation of B lymphocytes

as alternative strategies for regulating adaptive immune responses. *Nature communications*, *4*(1), 1-10.

Diamond, M. S., Staunton, D. E., Marlin, S. D., & Springer, T. A. (1991). Binding of the integrin Mac-1 (CD11b/CD18) to the third immunoglobulin-like domain of ICAM-1 (CD54) and its regulation by glycosylation. *Cell*, *65*(6), 961-971.

Medina-Leyte, D. J., Domínguez-Pérez, M., Mercado, I., Villarreal-Molina, M. T., & Jacobo-Albavera, L. (2020). Use of human umbilical vein endothelial cells (HUVEC) as a model to study cardiovascular disease: A review. *Applied Sciences*, *10*(3), 938.

Chen, Y. Y., Chen, J., Hu, J. W., Yang, Z. L., & Shen, Y. L. (2013). Enhancement of lipopolysaccharide-induced toll-like receptor 2 expression and inflammatory cytokine secretion in HUVECs under high glucose conditions. *Life sciences*, *92*(10), 582-588.

Dianzani, U., & Malavasi, F. (1995). Lymphocyte adhesion to endothelium. *Critical Reviews™ in Immunology*, *15*(2).

Leeuwenberg, J. F., Smeets, E. F., Neefjes, J. J., Shaffer, M. A., Cinek, T., Jeunhomme, T. M., ... & Buurman, W. A. (1992). E-selectin and intercellular adhesion molecule-1 are released by activated human endothelial cells in *vitro*. *Immunology*, *77*(4), 543.

Zhou, Z., Liu, Y., Miao, A. D., & Wang, S. Q. (2005). Protocatechuic aldehyde suppresses TNF-α-induced ICAM-1 and VCAM-1 expression in human umbilical vein endothelial cells. *European journal of pharmacology*, *513*(1-2), 1-8.

McDonald, B., & Kubes, P. (2015). Interactions between CD44 and hyaluronan in leukocyte trafficking. Frontiers in immunology, 6, 68.

Schubert, K. M., Qiu, J., Blodow, S., Wiedenmann, M., Lubomirov, L. T., Pfitzer, G., ... & Schneider, H. (2017). The AMP-related kinase (AMPK) induces Ca2+-independent dilation of resistance arteries by interfering with actin filament formation. Circulation research, 121(2), 149-161.

Alonzi, T., Agrati, C., Costabile, B., Cicchini, C., Amicone, L., Cavallari, C., ... & La Monica, N. (2004). Steatosis and intrahepatic lymphocyte recruitment

in hepatitis C virus transgenic mice. Journal of general virology, 85(6), 1509-1520.

Acknowledgements

First of all, I would like to thank my supervisor Prof. Dr. med. Markus Sperandio for giving me the opportunity to do my MD program in the lab and for his good ideas and guidance throughout the project.

Secondly, I would like to thank PD Dr. Heike Beck for her supervision and encouragement during the entire period of my MD study. I would also like to thank the members in our lab and the institute for their help and advice.

Besides, I would further like to thank Prof. Dr. Ulrich Pohl for giving me the opportunity to stay in Munich.

Also, I would like to thank the China Scholarship Council for the financial support during the entire period of my study in Germany.

Last but not least, I would like to thank my wife Na Li. You gave me the best support and encouragement. Although you may not understand much about biomedicine, you were always the best listener and gave me the best advices.

LMU LUDWIG-MAXIMILIANS-UNIVERSITÄT MÜNCHEN

Dean's Office
Faculty of Medicine

MMRS MUNICH MEDICAL RESEARCH SCHOOL

Affidavit

Cui,Ruicen

Surname, first name

Street

Zip code, town

Country

I hereby declare, that the submitted thesis entitled

The function of TDP-43 in lymphocyte recruitment

is my own work. I have only used the sources indicated and have not made unauthorised use of services of a third party. Where the work of others has been quoted or reproduced, the source is always given.

I further declare that the submitted thesis or parts thereof have not been presented as part of an examination degree to any other university.

Munich,30.11.2021

Place, date

Ruicen Cui

Signature doctoral candidate